RESEARCH ARTICLE SUMMARY

PSYCHENCODE2

Single-cell multi-cohort dissection of the schizophrenia transcriptome

W. Brad Ruzicka*†, Shahin Mohammadi†, John F. Fullard†, Jose Davila-Velderrain†, Sivan Subburaju, Daniel Reed Tso, Makayla Hourihan, Shan Jiang, Hao-Chih Lee, Jaroslav Bendl, PsychENCODE Consortium, Georgios Voloudakis, Vahram Haroutunian, Gabriel E. Hoffman, Panos Roussos*¶, Manolis Kellis*¶

INTRODUCTION: Schizophrenia population genomics has identified strong germline genetic associations for this highly heritable disorder, and molecular investigation of postmortem brain samples has yielded evidence of transcriptomic and epigenomic alterations associated with this disease. However, identifying molecular and cellular pathophysiological processes linking etiological risk factors and clinical presentation remains a challenge, due in part to the complex cellular architecture of the brain.

RATIONALE: Past work has implicated specific populations of excitatory and inhibitory neurons in the pathophysiology of schizophrenia, but existing large transcriptomic datasets of bulk tissue samples cannot directly assess cell type–specific contributions to disease. Single-cell RNA sequencing technologies allow measurement of genome-wide gene expression in individual cells with high-throughput, moving beyond bulk tissue measures to map disease-associated transcriptional changes in discrete cellular populations without bias toward preselected cell types. Investigating disease-associated phenotypic changes across the myriad cellular populations of the human brain can produce new insights into neuropsychiatric disease biology.

RESULTS: Using multiplexed single-nucleus RNA sequencing, we developed a single-cell resolution transcriptomic atlas of the prefrontal cortex across subjects with and without schizophrenia and present data from 468,727 nuclei isolated from 140 individuals across two well-defined and independently assayed cohorts. We identified expression profiles of brain cell types and neuronal subpopulations and systematically characterized the transcriptional changes associated with schizophrenia in each. For completeness, we report independent, cohort-specific analyses and joint meta-analysis of differential expression across 25 cell types. Using these data, we identified highly cell type–specific and reproducible expression changes, with 6634 differential expression events affecting 2455 genes and favoring down-regulated gene expression within excitatory neuronal populations. We found significant overlap with previously reported bulk cortex expression changes, primarily for excitatory neuronal populations, whereas changes in lower-abundance cell types were less efficiently captured in tissue-level profiling. Differentially expressed genes enrich neurodevelopmental and synapse-related molecular pathways and point to a regulatory core of coexpressed transcription factors linked to genetic risk variants for schizophrenia and developmental delay. Transcription factor targeting of schizophrenia differentially expressed genes in neuronal populations was validated with CUT&Tag in neuronal nuclei isolated from human prefrontal cortex. Furthermore, both transcriptional changes and putative upstream regulatory factors were enriched with genes harboring common and rare risk variants for schizophrenia, presenting evidence that genetic risk variants across the population frequency spectrum tend to target genes with measurable expression alterations in the excitatory neurons of patients with schizophrenia. Finally, the magnitude of schizophrenia-associated transcriptomic change segregated two populations of schizophrenia subjects. Transcriptomic heterogeneity within the cohorts was associated with specific cellular states shared across multiple neuronal populations, marked by genes related to synaptic function and one-carbon metabolism, suggesting genes characterizing distinct molecular phenotypes of schizophrenia.

CONCLUSION: Our results provide a valuable resource to investigate the molecular pathophysiology of schizophrenia at single-cell resolution, offering insights into preferential dysregulation of specific neuronal populations and their potential role in mediating genetic risk. Together, they suggest convergence of etiological genetic risk factors, neuronal transcriptional dysregulation, and symptomatic manifestation in schizophrenia. ■

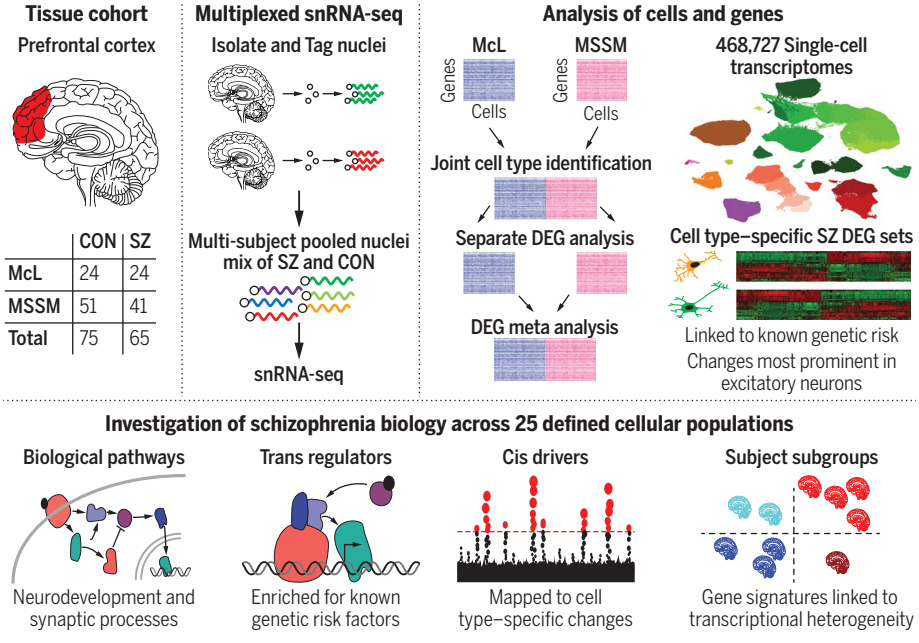

Single-cell schizophrenia transcriptomics. Single-nucleus RNA sequencing (snRNA-seq) identified cell type–specific differentially expressed genes (DEGs) in 25 cell types. DEG sets enrich disease-relevant biological pathways, implicate a coherently expressed transcription factors module, and are associated with schizophrenia genetic risk variants. Magnitude of transcriptional change identified neuronal cell state–associated subgroups. SZ, schizophrenia; CON, control; McL, McLean; MSSM, Mount Sinai School of Medicine.

The list of author affiliations is available in the full article online.
*Corresponding author. Email: wruzicka@mclean.harvard.edu (W.B.R.); panagiotis.roussos@mssm.edu (P.R.); manoli@mit.edu (M.K.)
†These authors contributed equally to this work.
¶These authors contributed equally to this work.
Cite this article as W. B. Ruzicka *et al.*, *Science* **384**, eadg5136 (2024). DOI: 10.1126/science.adg5136

READ THE FULL ARTICLE AT
https://doi.org/10.1126/science.adg5136

Corrected 6 August 2024. See full text.

RESEARCH ARTICLE

PSYCHENCODE2

Single-cell multi-cohort dissection of the schizophrenia transcriptome

W. Brad Ruzicka[1,2,3]*†, Shahin Mohammadi[3,4]†‡, John F. Fullard[5,6,7,8]†, Jose Davila-Velderrain[3,4,9]†, Sivan Subburaju[1,2], Daniel Reed Tso[1], Makayla Hourihan[1], Shan Jiang[6,7], Hao-Chih Lee[6,7], Jaroslav Bendl[5,6,7,8], PsychENCODE Consortium§, Georgios Voloudakis[5,6,7,8], Vahram Haroutunian[8,10], Gabriel E. Hoffman[5,6,7,8], Panos Roussos[5,6,7,8,9]*¶, Manolis Kellis[3,4]*¶

The complexity and heterogeneity of schizophrenia have hindered mechanistic elucidation and the development of more effective therapies. Here, we performed single-cell dissection of schizophrenia-associated transcriptomic changes in the human prefrontal cortex across 140 individuals in two independent cohorts. Excitatory neurons were the most affected cell group, with transcriptional changes converging on neurodevelopment and synapse-related molecular pathways. Transcriptional alterations included known genetic risk factors, suggesting convergence of rare and common genomic variants on neuronal population-specific alterations in schizophrenia. Based on the magnitude of schizophrenia-associated transcriptional change, we identified two populations of individuals with schizophrenia marked by expression of specific excitatory and inhibitory neuronal cell states. This single-cell atlas links transcriptomic changes to etiological genetic risk factors, contextualizing established knowledge within the human cortical cytoarchitecture and facilitating mechanistic understanding of schizophrenia pathophysiology and heterogeneity.

Schizophrenia is a neuropsychiatric disorder clinically characterized by a combination of psychosis, social withdrawal, and cognitive dysfunction, often leading to profound and chronic disability (*1*). Its pathogenesis is hypothesized to begin during prenatal brain development, yet first psychotic episodes do not occur until late in the second or early in the third decade of life (*2*). The complex etiology of schizophrenia involves genetic and environmental factors presumed to affect a wide range of brain-related processes, including neurodevelopment (*3*), synaptic function (*4*, *5*), neuronal excitability (*6*, *7*), neuronal connectivity (*8*, *9*), and cognition (*10*, *11*). Despite substantial advances in knowledge of the genetic basis of schizophrenia (*12*, *13*) and the functional genomic examination of postmortem tissue (*14*–*23*), elucidating specific molecular and cellular alterations linking etiological risk factors and clinical presentation remains challenging.

Cell type–specific molecular changes in schizophrenia have been previously reported with the use of targeted methods such as laser microdissection (*14*–*19*) and fluorescence-activated cell sorting (*22*, *23*), suggesting selective transcriptional vulnerability of deep-layer excitatory and parvalbumin-expressing interneurons. Although these approaches have revealed much about schizophrenia molecular pathophysiology, limitations include their reliance on marker gene expression to select cells of interest, limited ability to dissect subpopulations of major cell types, and the preselection of target cell types. Emerging technologies for single-cell transcriptomics (*24*, *25*) can achieve cell-type specificity without such biases, enabling the discovery of disease-associated changes as recently demonstrated for Alzheimer's disease (AD) (*26*), autism spectrum disorder (ASD) (*27*), major depressive disorder (MDD) (*28*, *29*), and multiple sclerosis (*30*).

To investigate cell types within the complex cytoarchitecture of the human brain presenting reproducible expression changes associated with schizophrenia, we profiled postmortem prefrontal cortex (PFC) tissue samples from two independent cohorts using single-nucleus RNA sequencing (snRNA-seq) (Fig. 1A). The McLean (McL) cohort included 24 individuals with schizophrenia and 24 healthy individuals, balanced for sex (12 males and 12 females per group), age (ranging from 22 to 94 years, average 63.5 years), and postmortem interval (ranging from 6.9 to 26.3 hours, average 16.8 hours). The Mount Sinai School of Medicine (MSSM) cohort included 41 individuals with schizophrenia and 51 healthy controls, balanced for age (ranging from 24 to 101 years, average 72.7 years) and postmortem interval (ranging from 2.0 to 52.8 hours, average 18.1 hours), including both males (61) and females (31) (fig. S1 and datafile S1). To increase the number of cells captured from each individual while reducing batch effects, we implemented a multiplexing strategy pooling a mixture of cases and controls in each sequencing library (see materials and methods for details). We report a total of 468,727 high-quality single-nucleus transcriptomes, including 206,014 nuclei from individuals with schizophrenia and 262,713 from healthy individuals, profiled at an average depth of 12,000 cells per individual and 35,000 reads per cell (McL) or 1200 cells per individual and 58,000 reads per cell (MSSM) (datafile S2). We used these data for the remainder of the study.

Identification of cellular populations across cohorts

We identified major brain cell types and neuronal subpopulations across both cohorts by building and annotating a cell similarity network using ACTIONet (*31*). Major brain cell classes, including excitatory and inhibitory neurons, astrocytes (Ast), oligodendrocytes (Oli), oligodendrocyte progenitor cells (OPCs), and microglia (Mic), were identified by preferential expression of known marker genes. By extracting and clustering each major cell class, we identified additional low-abundance cell types and neuronal subpopulations for a total of 27 cell types and subpopulations, capturing all major cell classes of the human PFC, including excitatory and inhibitory neuron subtypes and glial cells, with cell types well-represented across samples and cohorts (Fig. 1B and figs. S2 to S4). Excitatory neuronal subpopulations preferentially expressed cortical layer marker genes and were annotated accordingly (Fig. 1C and datafile S3). All annotations were consistent with expression patterns of selected marker genes across the cell similarity network (Fig. 1D). Neuronal subtypes, and excitatory neurons in particular, had higher numbers of expressed genes and unique molecular identifiers (UMIs) compared to non-neuronal cell types (figs. S5 to S7), consistent with previous observations (*26*, *27*).

Neuronal cells showed higher transcriptional diversity than glial cell types, and excitatory neuronal populations exhibited strong layer specificity. Within cortical layers V and VI, we identified three distinct populations of excitatory neurons: corticofugal projection neurons

[1]Laboratory for Epigenomics in Human Psychopathology, McLean Hospital, Belmont, MA 02478, USA. [2]Department of Psychiatry, Harvard Medical School, Boston, MA 02115, USA. [3]Broad Institute of MIT and Harvard, Cambridge, MA 02142, USA. [4]Computer Science and Artificial Intelligence Laboratory, Massachusetts Institute of Technology, Cambridge, MA 02139, USA. [5]Center for Disease Neurogenomics, Icahn School of Medicine at Mount Sinai, New York, NY 10029, USA. [6]Department of Genetics and Genomic Sciences, Icahn School of Medicine at Mount Sinai, New York, NY 10029, USA. [7]Icahn Institute for Data Science and Genomic Technology, Icahn School of Medicine at Mount Sinai, New York, NY 10029, USA. [8]Department of Psychiatry, Icahn School of Medicine at Mount Sinai, New York, NY 10029, USA. [9]Neurogenomics Research Center, Human Technopole, 20157 Milan, Italy. [10]Mental Illness Research, Education and Clinical Centers, James J. Peters VA Medical Center, Bronx, NY 10468, USA.
*Corresponding author. Email: wruzicka@mclean.harvard.edu (W.B.R.); panagiotis.roussos@mssm.edu (P.R.); manoli@mit.edu (M.K.)
†These authors contributed equally to this work.
‡Present address: insitro, South San Francisco, CA 94080, USA.
§PsychENCODE Consortium authors and affiliations are listed in the supplementary materials.
¶These authors contributed equally to this work.

Corrected 6 August 2024. See full text.

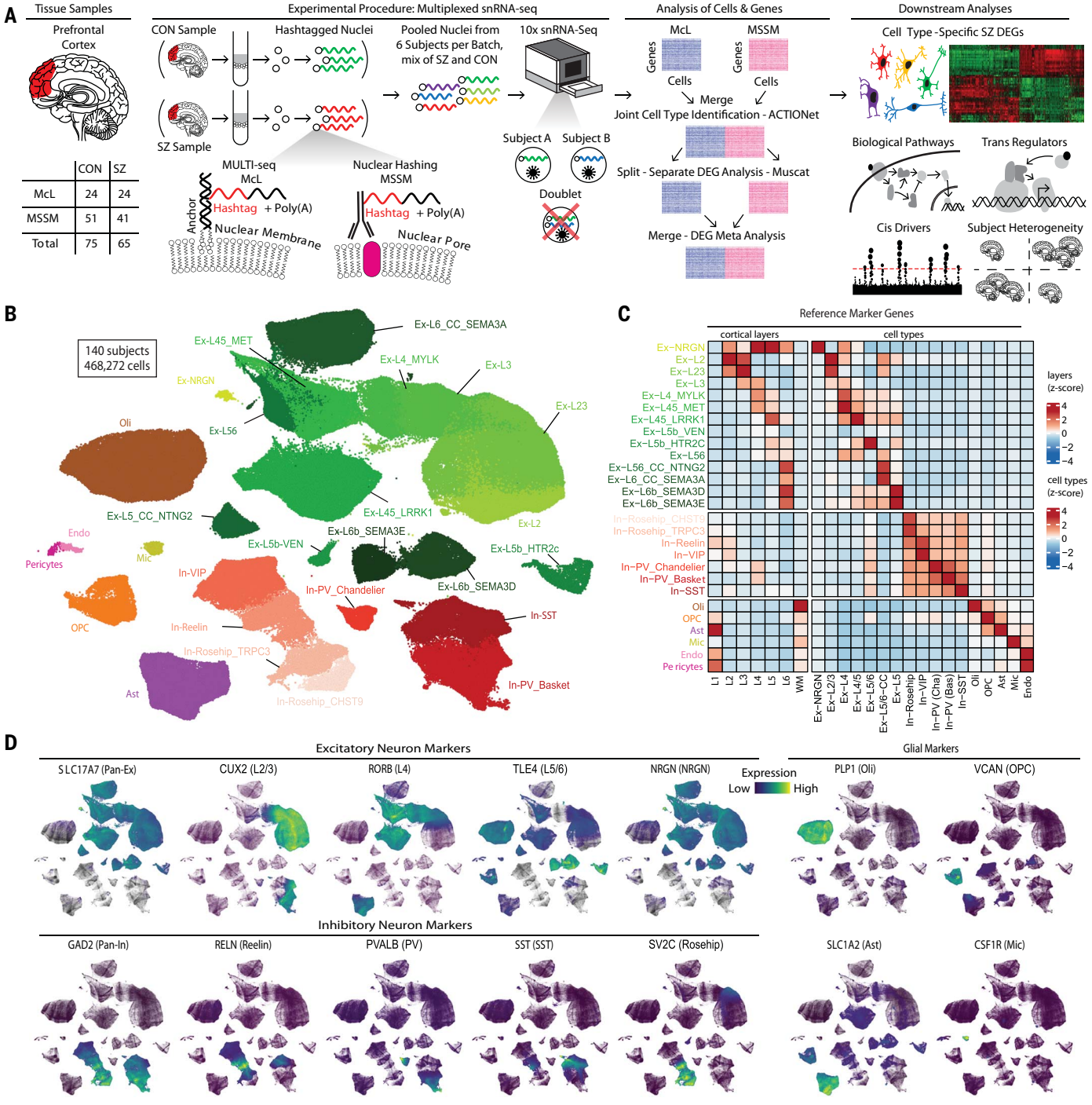

Fig. 1. Multiresolution dissection of cellular subpopulations. (**A**) Overview of study design and data analysis strategies. Nuclei were pooled after sample-specific hashtag labeling, allowing removal of intersample doublets. Cell annotation was performed on the combined dataset. DE analysis was performed within each dataset independently and results merged through meta-analysis. Downstream analyses of biological pathways and cis- and trans-regulatory factors related to cell type–specific schizophrenia DEGs (right). CON, control; SZ, schizophrenia; McL, McLean cohort; MSSM, Mount Sinai School of Medicine cohort. (**B**) ACTIONet plot of putative cell types. Green and red clusters represent excitatory and inhibitory subtypes of neurons, respectively, with darker shades indicating an association with deeper cortical layers. (**C**) Annotation of cell types using curated markers (*31*) from previous snRNA-seq (*26*, *27*, *79*) and spatial transcriptomics (*38*) studies. (**D**) Projection of known marker genes verifies cell-type annotations and cortical layer associations (*85*).

(Ex-L5/6) expressing *FEZF2*, and two distinct populations of cortico-cortical projection neurons expressing *NTNG2* (Ex-L56_CC_NTNG2) and *SEMA3A* (Ex-L6_CC_SEMA3A) (Fig. 1B).

γ-Aminobutyric acid (GABA)–mediated inhibitory neurons are organized in major subtypes, including neurons expressing parvalbumin (*PV*), neuropeptide somatostatin (*SST*), and the ionotropic serotonin receptor (5HT3aR). Within these groups, we detected two PV-expressing subtypes of inhibitory neurons (basket and chandelier cells), two 5HT3aR-expressing subtypes

Corrected 6 August 2024. See full text.

[vasoactive intestinal peptide (VIP)+ and Reelin+], and two subpopulations of the recently described rosehip interneurons (*32*). We validated this heterogeneity within rosehip interneurons using in situ hybridization (fig. S8). The relative position of cells within the cell similarity network is consistent with the developmental origin of cardinal interneuron subtypes (medial versus caudal ganglionic eminence), suggesting a developmental basis for shared transcriptional signatures (*33*).

Prior histologic studies have suggested loss of cells within inhibitory neuronal populations in schizophrenia (*34*), with much attention focused on PV-expressing interneurons (*35*). These studies were performed using histology-based cell-counting techniques, and the detected neuronal loss might have been due to technical limitations, where marker expression fell below the level of histological detection without loss of cells (*36*). The current data generated by the unbiased sampling of cells across all cortical layers support this hypothesis, as we detected no change in the representation of any cell type, including all subtypes of inhibitory neurons, between individuals with schizophrenia and healthy individuals (fig. S4B). A recent snRNA-seq study of dorsolateral PFC in a smaller cohort (9 schizophrenia, 14 healthy individuals) did observe a decrease in multiple inhibitory neuronal cell types (*37*).

Cell type–specific expression changes in schizophrenia

To identify transcriptional alterations associated with schizophrenia, we systematically performed differential expression (DE) analysis for each cell type in each cohort separately, and subsequently performed a meta-analysis to integrate the results (see materials and methods for details). Meta-analysis identified a total of 6634 DE events [false-discovery rate (FDR) < 0.05 and $|\log_2(\text{fold change})| > 0.1$, 2455 unique differentially expressed genes (DEGs)] across all cell types, most of which (77%, $n = 5141$) were down-regulated in schizophrenia (Fig. 2A and datafile S4). Changes occurred predominantly in neuronal populations (94%, $n = 6229$) and mostly in excitatory neurons (77%, $n = 5129$). Overall, DEGs were reproducible across datasets (Fig. 2B), with 745 genes consistently detected as up-regulated or down-regulated in both cohorts independently. Cross-cohort DEG reproducibility varied across cell types and was highest for excitatory neurons. DEGs identified by means of meta-analysis overlapped with those identified in each cohort separately, supporting the data integration procedure (Fig. 2B, fig. S9, and table S1). We report cohort-specific analyses, a joint meta-analysis of DE across 25 cell types, and a highly reproducible set of 287 DEGs with consistent expression changes in all three analyses (datafile S5).

Comparative analysis with schizophrenia DEGs identified in high-quality bulk cortex RNA-seq data from the PsychENCODE consortium (559 individuals with schizophrenia versus 936 healthy individuals finding 4821 DEGs with FDR < 0.05) (*20*) validated the DEGs that we identified in our snRNA-seq data, with high concordance of expression changes, especially with those observed in neurons. Enrichment analysis revealed that bulk data primarily captured expression changes observed at the single-cell level in excitatory neurons, astrocytes, and oligodendrocytes (Fig. 2C). Changes in other cell types, including inhibitory neurons, were less well-captured in bulk, highlighting the relevance of performing single-cell assessments.

Most up-regulated DEGs occurred in excitatory neurons of the superficial cortical layers, whereas most down-regulation events occurred in deep-layer excitatory neurons, consistent with prior mapping of bulk schizophrenia DEGs to cortical layers based on spatial transcriptomics (*38*) (Fig. 2A). Predominance of transcriptional changes in excitatory neurons is consistent with prior work (*39*) and is robust to confounding by variability in the number of cells captured per cell type, as demonstrated by lack of correlation between the number of cells and the number of DEGs in each cell type, and by downsampling of the most abundant neuronal population, Ex-L23 (table S2 and fig. S10). Nearly half of DEGs were altered in just one cell type (47%, $n = 1153$), indicating high cell-type specificity of expression changes. Schizophrenia cell type–specific DEGs did not overlap with genes responsive to chronic antipsychotic exposure in nonhuman primates (*21*) (fig. S11), suggesting that identified expression changes are not driven by medication exposure.

Among 1302 genes dysregulated in multiple cell types, 114 genes showed divergent directionality of changes across cell populations. The most broadly divergently dysregulated genes included *NRXN3*, *PFKFB3*, *RASGRF2*, *SHANK2*, and *DLG5*, all previously associated with schizophrenia by functional or genetic data (*20*, *40*–*44*). Our single-cell resolution data indicate that alterations in these genes tend to occur in a single direction within and divergently across cell classes (excitatory, inhibitory, and glial), suggesting that cell type–specific regulatory complexity may be relevant for gene expression modulation (Fig. 2D and fig. S12A). Overrepresentation of genes involved in synaptic structure and function further suggests the biological relevance of divergent dysregulation across neuronal classes (fig. S12B).

DEGs affect neurodevelopment and synapse-related pathways

To determine the biological pathways affected by these cell type–specific DEGs, we performed gene ontology analysis for the 50 down-regulated or up-regulated DEG sets and semantically clustered the significantly enriched terms into biological themes to aid interpretation. Expression changes converged to 14 biological themes summarizing functionally related molecular pathways, with neurodevelopmental and synaptic processes highly overrepresented within schizophrenia DEG associations (Fig. 2, E and F, and datafiles S6 and S7). Biological themes related to neurodevelopmental processes were associated with DEG sets within excitatory and inhibitory neuronal populations, with the terms "neuron development" and "plasma membrane–bound cell projection organization" most strongly enriched.

Within synapse-related processes, the theme "anterograde trans-synaptic signaling" was the most broadly dysregulated, associated with down-regulated DEG sets in 12 distinct neuronal populations and with up-regulated DEG sets in Ex-L23. The theme "regulation of neurotransmitter receptor activity" was dysregulated within four populations of excitatory neurons and included more specific terms related to glutamatergic signaling through regulation of α-amino-3-hydroxy-5-methyl-4-isoxazolepropionic acid (AMPA) and *N*-methyl-D-aspartate (NMDA) receptors. We validated the down-regulation of seven genes broadly represented across multiple pathways within these synapse-relevant themes (*BCR*, *BSN*, *NEURL1*, *PSEN1*, *RASGRF1*, *SHANK2*, *SLC1A2*) with quantitative polymerase chain reaction (qPCR) with reverse transcription (qPCR, fig. S13). All seven genes were found to be down-regulated in schizophrenia when comparing RNA extracted from whole-cortex postmortem BA10 tissue from 12 individuals with schizophrenia versus 11 healthy individuals (McLean cohort).

Ex-L23 up-regulated DEGs enriched the greatest number of themes (6 of 14), consistent with having the largest number of up-regulated DEGs, whereas down-regulated DEGs within Ex-L2 and Ex-L6_SEMA3A enriched the greatest number of themes (9 of 14), despite Ex-L2 having less than half the number of down-regulated DEGs as some deep-layer excitatory populations. Inhibitory neurons showed more modest alteration of these themes, with synaptic signaling enriched by down-regulated DEGs in In-Rosehip_TRPC3 and In-Reelin, and neurodevelopment relevant terms enriched by up-regulated DEGs in In-Rosehip_TRPC3. Altogether, our data suggest that schizophrenia DEGs converge on functionally related molecular pathways, with the strongest evidence implicating neurodevelopmental, synaptic, and intracellular signaling–relevant processes.

Considering the abundance of dysregulated pathways related to synaptic structure and function, we investigated enrichment of synaptic compartment genes within DEGs across cell types as annotated in the SynGO database

Corrected 6 August 2024. See full text.

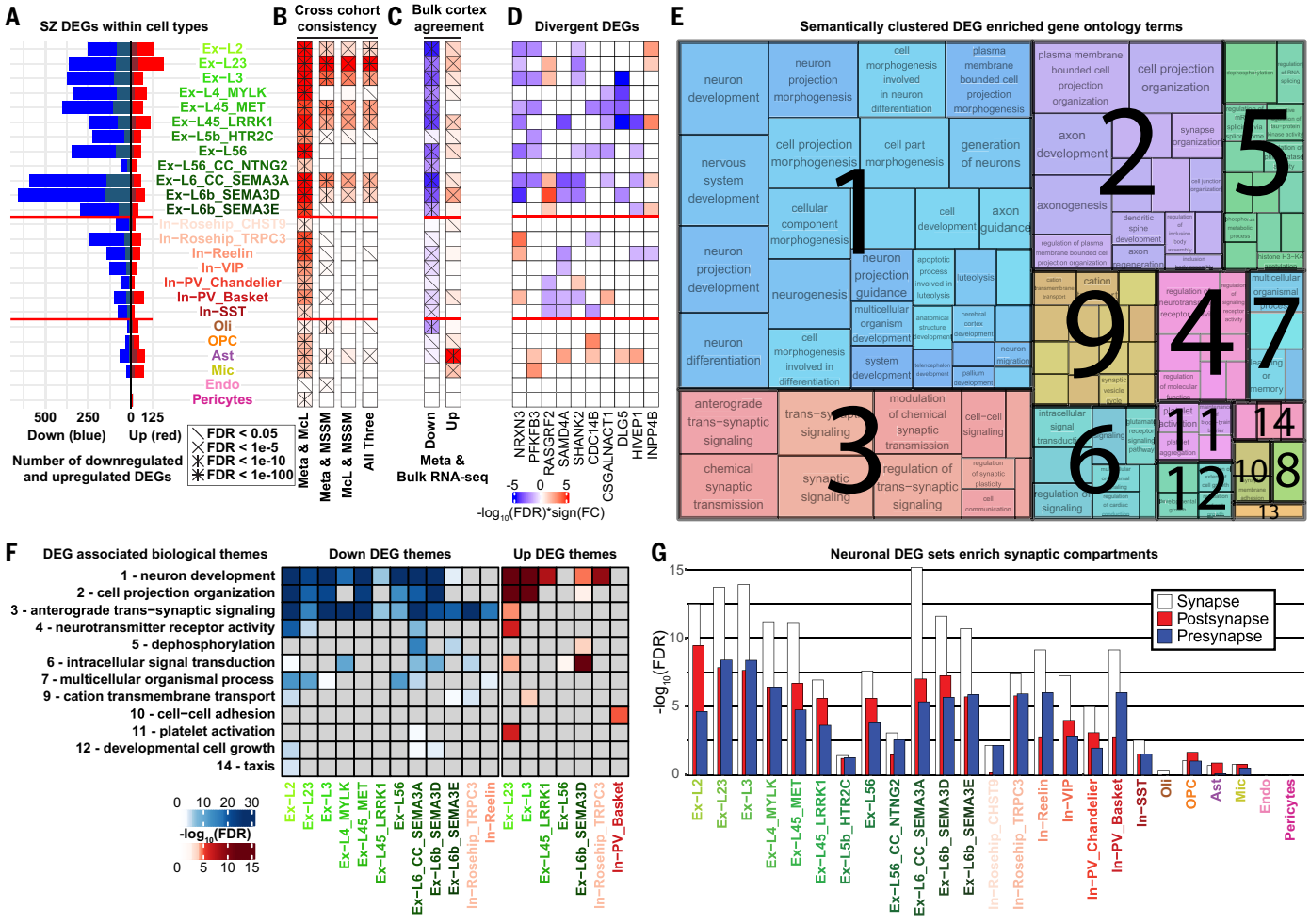

Fig. 2. Cell type–specific DEGs and associated biological pathways in schizophrenia. (**A**) Number of down-regulated (blue, left of 0) and up-regulated (red, right of 0) genes with FDR < 0.05 and abs($\log_2$(fold change)) > 0.1 in meta-analysis combining results of both cohorts. Shaded regions of each bar indicate the number of genes also significantly different with the same direction of change in a bulk tissue RNA-seq study of schizophrenia PFC (*20*). (**B**) Significance of overlap between cell type–specific DEG sets identified in each cohort and in the meta-analysis, computed with the R package SuperExactTest (*48*). Columns are scaled independently with darker color indicating greater significance of overlap, and cross hatches indicating the specific level of significance of each tested overlap. (**C**) Concordance of meta-analysis DEGs and DEGs identified by prior bulk cortex RNA-seq (*20*) with up- and down-regulated DEGs considered separately. Columns are scaled and highlighted as in (B). (**D**) Signed significance of DE for the 10 most broadly and divergently dysregulated genes. FC, fold change. (**E**) Biological pathways overrepresented within cell type–specific DEGs determined by gene set enrichment and semantic clustering analysis of gene ontology (GO) terms. A total of 119 enriched GO terms revealed 14 distinct biological themes listed in panel (F) and datafile S7. Numbers indicate significance rank. Themes are named by the most significant term they contain. (**F**) Aggregate enrichment of GO terms within each biological theme across cell types by down-regulated (blue) and up-regulated (red) DEGs, excluding themes implicated by only one term and nonsignificant cell types. (**G**) Overrepresentation of synaptic compartment genes [SynGO database (*45*)] within cell type–specific DEGs.

(*45*). We found the top-level SynGO compartment "synapse" to be significantly enriched (FDR < 0.05) across all neuronal cell types, and no non-neuronal cell types (Fig. 2G). Enrichment of the presynaptic and postsynaptic compartments was similar across neuronal populations, with a slight predominance of postsynaptic annotations for excitatory neuronal DEGs, and presynaptic annotations for inhibitory neuronal DEGs. Postsynaptic annotations were also enriched in OPCs. Results for all enriched SynGO compartments are available in datafile S8.

Neuronal DEGs are targets of schizophrenia GWAS risk transcription factors

Because coordinated expression changes are often driven by common upstream transcriptional regulators (*46*), we investigated whether observed cell type–specific dysregulation was associated with specific trans-acting factors. We grouped regulators with similar expression profiles by coexpression analysis (datafile S9 and fig. S14) and performed transcription factor (TF) target analysis to test for overrepresentation of target genes within schizophrenia DEGs, finding a single TF module that was highly associated with neuronal DEGs (TF module 10, Fig. 3A). This module includes 24 TFs coherently expressed and supported by protein-protein interactions documented in the literature, with 14 of these TFs linked in a highly connected interaction network supported by multiple lines of evidence within the STRING database (*47*) (Fig. 3B). TFs within this module overlap significantly with genes implicated by exome sequencing in neurodevelopmental delay [11 of 24 TFs in 373 genes, P = 4.7e-13, SuperExactTest (*48*)] and ASD (4 of 24 TFs in 72 genes, P = 2.3e-6) (*49*), and

Corrected 6 August 2024. See full text.

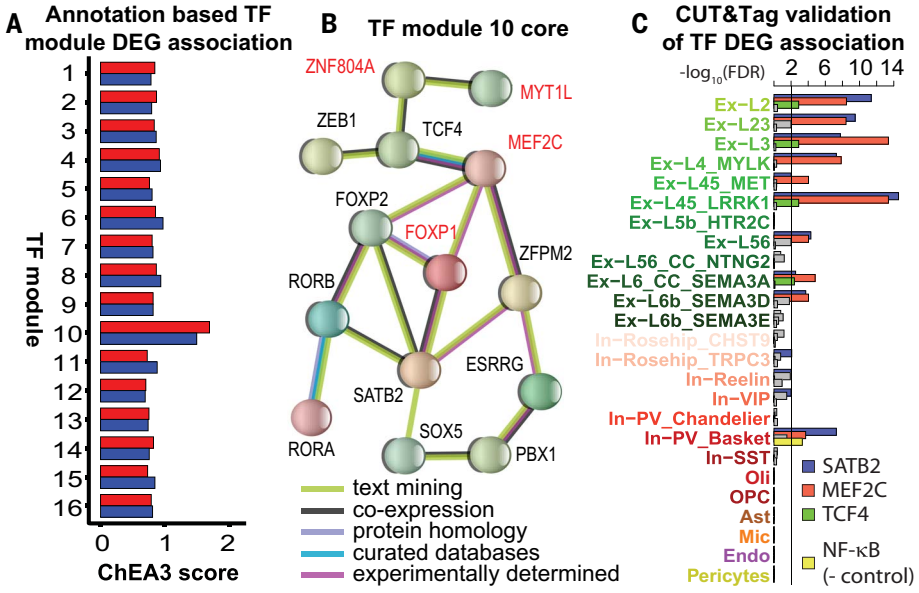

Fig. 3. Schizophrenia DEGs implicate a coherently expressed TF module. (**A**) Prioritization of TF coexpression modules by overrepresentation of annotated TF targets within DEGs performed using ChEA3 (*86*). Red bars depict ChEA3 enrichment scores for up-regulated DEGs and blue bars, for down-regulated DEGs. (**B**) TFs within module 10 form a highly connected protein-protein association network supported by multiple lines of evidence [STRING database (*47*)]. TFs named in red are fine-mapping prioritized schizophrenia risk genes reported by the Psychiatric Genomics Consortium (*12*). (**C**) Genomic loci bound by MEF2C, SATB2, or TCF4 in postmortem human PFC neurons are significantly associated with schizophrenia DEGs across multiple neuronal and no non-neuronal populations.

include multiple TFs (7 of 24) encoded by schizophrenia genome-wide association study (GWAS) risk genes (*12*).

To validate predicted associations between prioritized TFs and observed schizophrenia DEGs, we experimentally tested whether active cis-regulatory elements that are targeted by these TFs show preferential association with schizophrenia DEGs. We performed Cleavage Under Targets and Tagmentation [CUT&Tag (*50*)] assays in four healthy individuals within the McLean cohort to map the genome-wide binding of MEF2C, SATB2, and TCF4, and further included nuclear factor κB (NF-κB) as a negative control not expected to show strong association with schizophrenia DEGs. These assays were performed in neuronal nuclei isolated from postmortem PFC tissue samples using fluorescence-activated nuclear sorting. We defined reproducibly bound regions as those bound in at least 50% of replicates and annotated them with the nearest gene (datafile S10). Supporting the specificity of this analysis, genes targeted by MEF2C, SATB2, and TCF4 preferentially enrich biological pathways relevant to neuronal function (fig. S15). We found a high degree of overlap between identified target genes and schizophrenia DEGs across a wide range of excitatory neurons, and a lower degree of overlap within multiple inhibitory populations (Fig. 3C). We found no association in any non-neuronal cell type, again supporting the specificity of our analysis as CUT&Tag assays were performed only in neurons. Overall, these experimental data support a regulatory association between members of TF module 10 and cell type–specific schizophrenia dysregulated genes.

Schizophrenia DEGs are associated with common and rare genetic risk variants

Seeking insights into the association between transcriptional alterations and genetic liability to schizophrenia, we investigated the relationship between transcriptionally dysregulated genes and genetic risk loci. In this context, two questions are of relevance. First, genes that are dysregulated in schizophrenia may also be associated with genetic variation, suggesting a link between genetic liability and measurable cell type–specific molecular alterations. Second, genes that are preferentially expressed by specific cell types may, as a class, contribute to schizophrenia risk, suggesting a functional role of those cells in mediating genetic risk. We found strong evidence supporting the first scenario in most excitatory neurons, and only modest evidence for the second in superficial-layer neurons (Fig. 4A, fig. S16, and datafile S11). We used Hi-C-coupled MAGMA (H-MAGMA) (*51*) to compute gene-level genetic risk scores from GWAS summary statistics by assigning noncoding single-nucleotide polymorphisms (SNPs) to their cognate genes based on evidence of long-range interactions in the adult dorsolateral PFC (*52*) (see materials and methods for details). Genetic risk scores were significantly elevated for DEGs from most excitatory subpopulations as compared to randomly selected genes (Bonferroni-corrected $P < 0.01$, resampling test), with Ex-L6_CC_SEMA3A neurons showing the strongest effect. Notably, we did not observe similar elevations for preferentially expressed genes (PEGs, see materials and methods for details: gene specificity score), which showed only modest evidence for higher-than-expected GWAS risk scores (nominal $P < 0.01$). Consistent with these observations, GWAS scores of schizophrenia DEGs overall were higher than those of PEGs in the same cell type (nominal $P < 0.05$ in most cell types, Bonferroni-corrected $P < 0.01$ in deep-layer excitatory neurons). We obtained similar results with greater association of both DEGs and PEGs with GWAS risk using gene-level genetic risk scores computed with standard MAGMA (*53*) (fig. S16).

Past efforts have identified potential cell types affected by disease-associated genetic variants by assigning schizophrenia risk genes to cell types that preferentially express them in neurotypical brains (*12*, *39*), implicating specific neuronal populations within multiple regions of the prenatal human brain in mediating schizophrenia genetic risk (*54*). Our data support the merit of this approach, as preferentially expressed genes were more associated with genetic risk than are randomly selected genes in relevant neuronal subtypes. With the caveat that genetic risk loci may influence gene function through additional mechanisms beyond transcriptional dysregulation, and that transcriptional alterations observed in postmortem cortical samples of individuals with schizophrenia might stem from several direct and indirect mechanisms, our data complement previous findings (*20*) supporting a degree of convergence in genetic and transcriptional changes in schizophrenia that is largely cell type–specific.

To further investigate the association between transcriptional alterations and genetic liability to schizophrenia genome-wide, we tested the statistical association between aggregate gene-level genetic risk from common variants and cell type–specific expression alterations. In addition to schizophrenia (*12*), we further considered risk loci for three psychiatric disorders that are known to share genetic risk factors (*51*): MDD (*55*), bipolar disorder (BD) (*56*), and ASD (*57*). This approach allowed us to distinguish schizophrenia from general psychiatric illness–related associations. As a point of contrast, we included AD (*58*), a neurodegenerative disorder not expected to be genetically related to schizophrenia. Furthermore,

Corrected 6 August 2024. See full text.

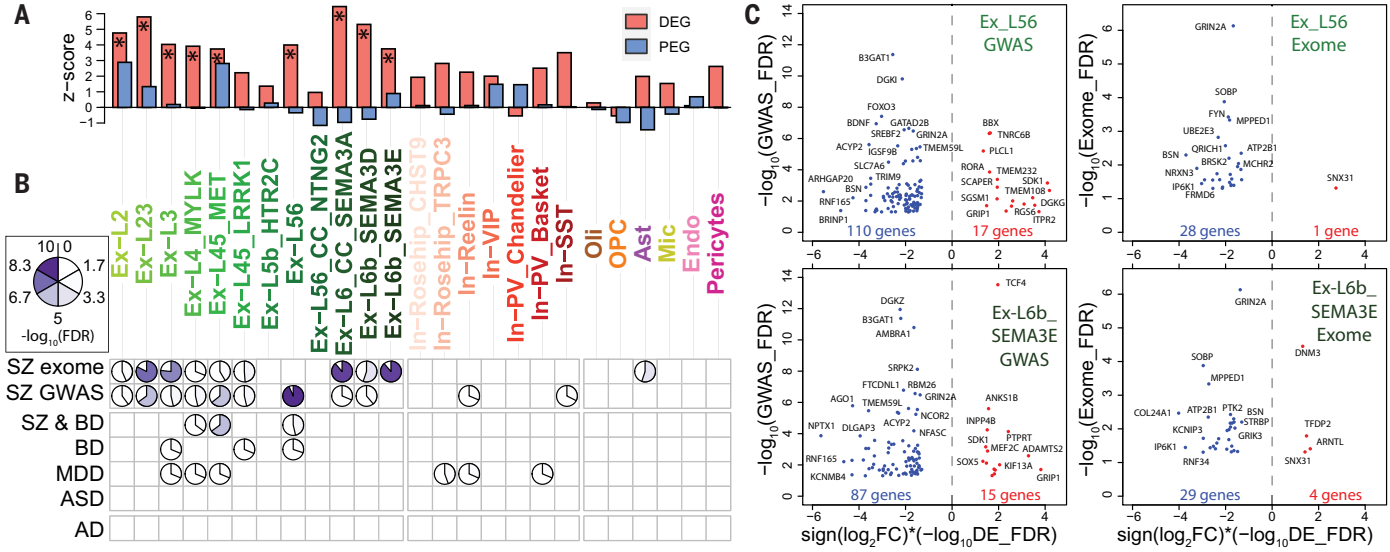

Fig. 4. Association of DEGs with genetic risk variants across cell types and disorders. (**A**) Enrichment of GWAS signal (gene-level scores computed with H-MAGMA; standard MAGMA results presented for comparison in fig. S16) within cell type–specific schizophrenia DEGs (red) and equal numbers of genes preferentially expressed in each cell type (PEG, blue) assessed by permutation test against randomly selected genes. Asterisks indicate significant deviation from random expectation (Bonferroni-corrected $P < 0.01$). PEGs do not significantly deviate from random expectation in any cell type. (**B**) Genome-wide association between cell type–specific schizophrenia differential expression and genomic variants implicated by GWAS across multiple neuropsychiatric disorders computed with H-MAGMA (*51*), and by exome sequencing for schizophrenia (*13*) (SZ exome) computed by gene set enrichment analysis (GSEA). Pie charts and fill color both indicate $-\log_{10}$(FDR). Empty tiles indicate no significant association (FDR > 0.01). (**C**) Visualization of genes most strongly associated (FDR < 0.05) with common schizophrenia risk variants (GWAS) computed with H-MAGMA (*y* axis, left), or rare schizophrenia risk variants (exome sequencing, *y* axis, right), with significant expression changes in schizophrenia (*x* axis) within excitatory neuronal populations showing the strongest associations in panel (B).

to extend associations beyond common, small-effect variants, we also considered schizophrenia-associated rare protein-coding variants (*13*).

We found strong associations between schizophrenia DEGs and genes targeted by common or rare risk variants in multiple neuronal subpopulations, supporting a link between genetic liability and observed transcriptional alterations (Fig. 4B). Across excitatory neuronal subpopulations, the observed layer specificity of these associations was again consistent with the enrichment of schizophrenia genetic variants proximal to PEGs in layers II and V (*38*). Whereas common and rare risk variants were associated with transcriptional change in a highly overlapping set of excitatory neuronal populations, separations did occur, with Ex-L56 DEGs being the most associated with common variants, but not associated with rare protein-coding mutations. Conversely, Ex-L6b_SEMA3E transcriptional change displayed the strongest association with rare variants but was not enriched with common variants. Because the gene sets and biological processes affected by common and rare variants are thought to be highly overlapping (*13*), the divergence of excitatory neuronal populations showing expression changes in associated genes observed here might be relevant for understanding how the outcomes of distinct categories of genetic risk factors are partitioned across the cortical cytoarchitecture.

We found that some of the cell types whose transcriptional perturbations show a strong association with schizophrenia genetic risk variants are also associated with risk variants for BD and MDD, which is consistent with their previously reported strong genetic relationships, both at the level of genetic correlations and gene-level overlaps (*51*, *59*). We found no association between schizophrenia transcriptional changes and ASD risk, consistent with the known lower correlation of genetic risk between these disorders (*59*) (with the caveat that the ASD GWAS study on which this analysis is based is less well-powered than those used for other disorders). As expected, we found no overlap with genetic risk for AD.

We next examined specific genes with strong evidence of association with both genetic risk and DE within those neuronal populations showing convergent genetic and transcriptomic alterations. We found that several genes with strong evidence of association with common schizophrenia risk variants were consistently dysregulated across multiple populations, including *GATAD2B*, *DGKI* and *DGKZ*, *FXR1*, *HSPA1A*, and *TCF4* (Fig. 4C and fig. S17). Among the 32 genes associated with rare variants at FDR < 0.05, we found nine to be differentially expressed, primarily in excitatory neuronal populations, with only one gene (*ANKRD12*) dysregulated exclusively in a non-neuronal population (Fig. 4C and fig. S18). Of the 10 genes with exome-wide association, four (*GRIN2A*, *NRXN3*, *BSN*, and *SOBP*) were down-regulated in schizophrenia.

We next focused on genes linked to credible, common schizophrenia-associated variants and mapped their transcriptional dysregulation across cell populations within the human PFC. We found strong evidence of DE in at least one cell type for 110 protein-coding genes within the Psychiatric Genomics Consortium's "broad fine-mapped set" of schizophrenia risk genes (n = 628) (*12*) (Fig. 5). For 87 of these genes, the strongest schizophrenia DE event was observed in an excitatory neuronal population, whereas 20 were most robustly altered in inhibitory neurons, and 7 in non-neuronal populations. Of the 628 prioritized genes, 113 were dysregulated in a past assessment of bulk PFC (*20*), with 36 genes dysregulated in both the bulk cortex and the current single-cell study. The Psychiatric Genomics Consortium further refined its gene list using fine-mapping, summary-based Mendelian randomization, and expression quantitative trait loci (eQTL) colocalization analysis to prioritize 120 genes presumed to mediate schizophrenia risk, 31 of which were DEGs in the present study (Fig. 5).

Transcriptional pathology recovers heterogeneous schizophrenia subgroups

Schizophrenia is a highly heterogeneous disorder, with classical descriptions of multiple

Corrected 6 August 2024. See full text.

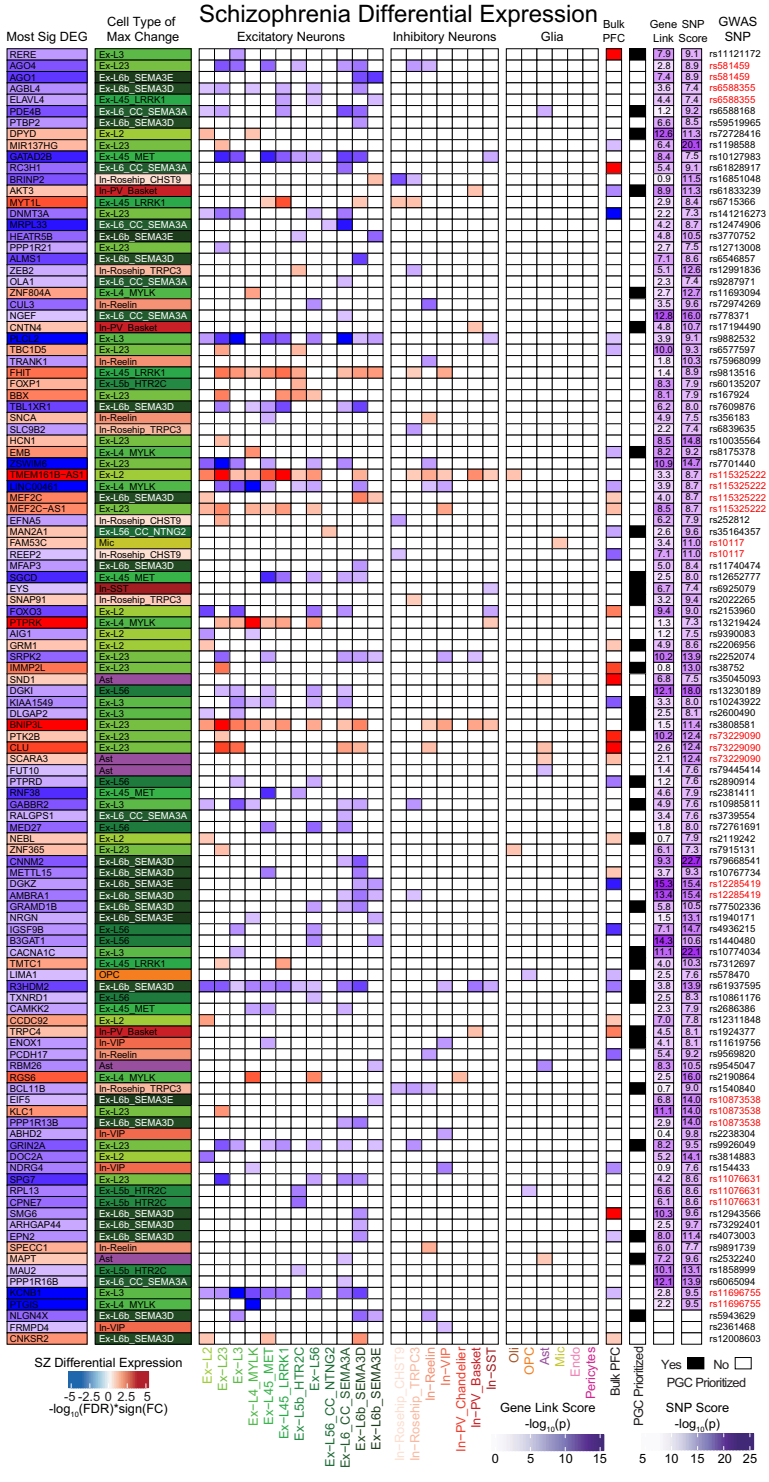

Fig. 5. Cell type–specific differential expression of high-confidence schizophrenia risk genes. Cell type–specific and bulk PFC differential expression of 114 genes within the Psychiatric Genomics Consortium's broad fine-mapped set (*12*). Shading indicates significance and direction of change (red, up-regulated; blue, down-regulated). Significance of association of each gene with schizophrenia common risk loci computed with H-MAGMA (Gene Link Score). Significance of the index SNP linked to each gene by the PGC3's statistical fine mapping (SNP Score). PGC prioritized indicates that the gene is present within the Psychiatric Genomics Consortium's set of 120 prioritized schizophrenia risk genes. Index SNPs in red are linked to multiple DEGs.

clinical subtypes and evidence of diverse etiology. To investigate whether such heterogeneity manifests at the transcriptomic level across cell types and individuals, we developed a transcriptional pathology score (TPS). TPS assesses the degree of consistency between the genome-wide gene expression of each individual (relative to the average across all individuals) and the expression changes observed between individuals with schizophrenia and healthy individuals, complementing the binary case versus control diagnosis with a continuous measure of transcriptomic change. A high TPS value indicates that the relative expression profile of an individual is globally consistent with the expression changes expected in schizophrenia compared to healthy individuals. TPS was calculated for each cell type separately, and each individual was assigned an aggregate TPS averaged across neuronal cell types (see materials and methods for details). By ranking all individuals by their aggregate TPS, we discovered four groups of individuals: individuals with schizophrenia that appear transcriptionally consistent with schizophrenia (SZ), individuals with schizophrenia that appear transcriptionally more similar to the healthy group (SZ_CON-like), healthy individuals that appear transcriptionally consistent with control (CON), and healthy individuals that appear transcriptionally more similar to the schizophrenia group (CON_SZ-like) (Fig. 6, A and B). This analysis indicates that clinical diagnosis and underlying transcriptional patterns are not always consistent, suggesting structured heterogeneity within diagnostic groups at the transcriptional level. In particular, a subset of individuals clinically diagnosed with schizophrenia does not present the expected transcriptional alterations observed across the whole cohort, consistent with prior studies of gene expression in bulk cortex (*60*).

TPS is computed on the basis of reference case-control expression changes. To test whether similar patterns of inconsistency between diagnosis and transcriptional pathology occur in both cohorts, we performed the following computational validation experiment. We classified individuals into subgroups based on TPS calculated using schizophrenia-associated expression changes observed only within the McL cohort, only within the MSSM cohort, or jointly in the cross-cohort meta-analysis, and then quantified group assignment consistency across these classifications. In all cases, we found significant overlap between individuals within each class ($P < 1.9e\text{-}19$, fig. S19), indicating that patterns of inconsistency between diagnosis and transcriptional pathology across individuals are reproducible in both cohorts (consistently classified individuals: SZ, 35; SZ_CON-like, 13, CON_SZ-like, 17; CON, 36). Individuals whose classification depended on

Corrected 6 August 2024. See full text.

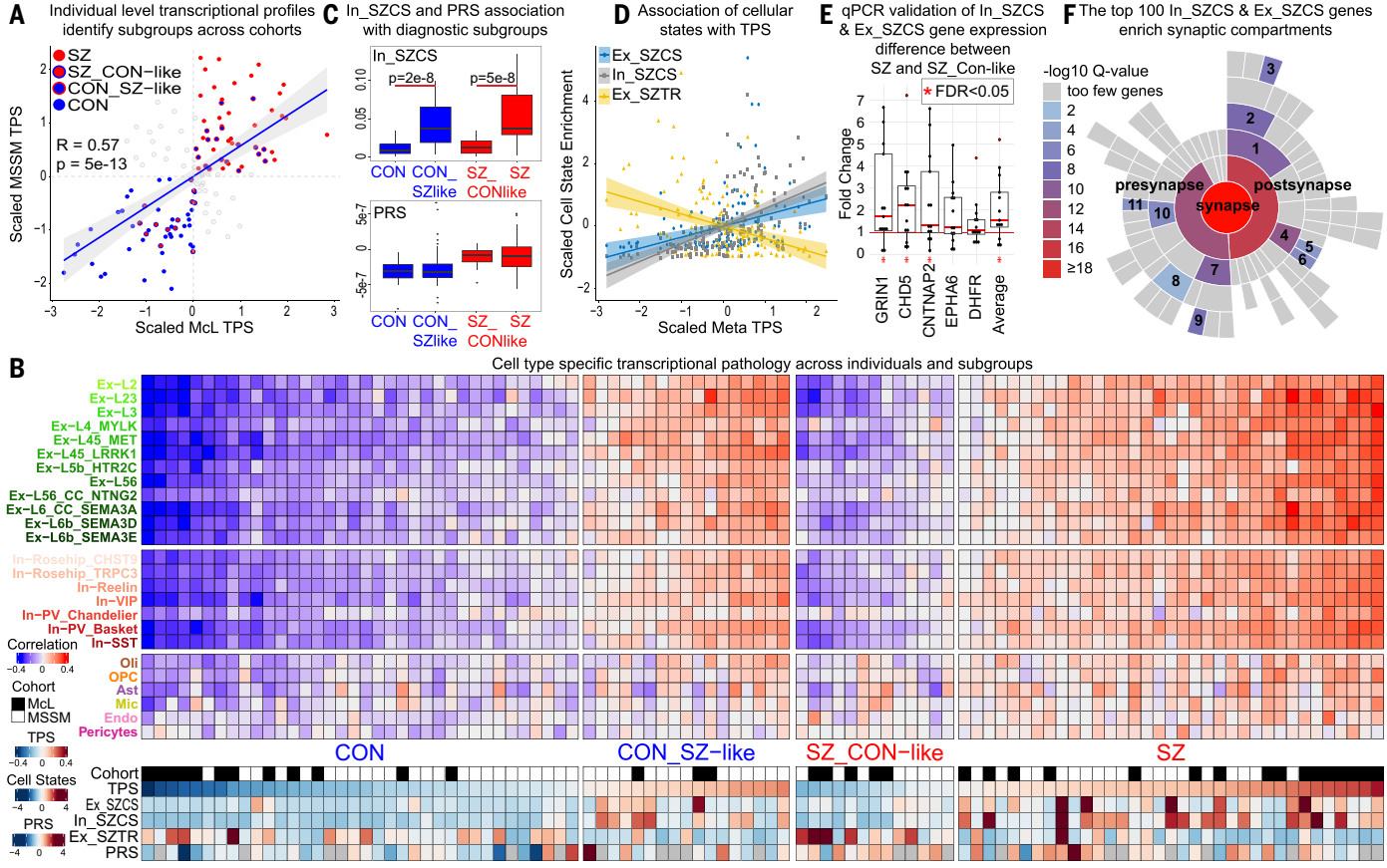

Fig. 6. Heterogeneity of transcriptional changes across individual subjects. (**A**) Individuals plotted by TPS computed within the space of schizophrenia-associated transcriptional change observed in the McL cohort (*x* axis) or the MSSM cohort (*y* axis). Values are scaled, with larger values indicating a greater association with schizophrenia. Four subgroups of individuals are identified: SZ, red points in the upper right quadrant; CON, blue points in the lower left quadrant; SZ_CON-like, red points outlined in blue in the lower left quadrant; and CON_SZ-like, blue points outlined in red in the upper right quadrant. Off-diagonal individuals (gray points) are inconsistently classified between analyses. R, Pearson correlation coefficient. Regression line computed using all data, including gray points. (**B**) TPS within individuals clustered into the four groups identified in panel (A). Values are scaled, with darker red indicating a value more characteristic of the schizophrenia group, and darker blue indicating a value more characteristic of the control group. Correlation, cell type–specific correlation between each individual's transcriptional signature and the transcriptional signature characteristic of the SZ group; TPS, Transcriptional Pathology Score averaged across neuronal cell types for each individual; Ex_SZCS, In_SZCS, Ex_SZTR, scaled expression of each transcriptional signature within each individual; PRS, schizophrenia polygenic risk score. Individuals with inconsistent classification in panel (A) were omitted from panel (B). (**C**) Enrichment of the In_SZCS transcriptional signature (top) within all individuals across the four groups identified in panel (A), showing a high association with diagnostic subgroups. PRS (bottom) does not show this association. (**D**) Correlation between cell-state transcriptional signatures and schizophrenia transcriptional change across individuals, with In_SZCS and Ex_SZCS showing positive (R = 0.56, P = 4.6e-13, and R = 0.35, P = 1.9e-5, respectively) and Ex_SZTR showing inverse association with TPS (R = −0.39, P = 1.8e-6). (**E**) qPCR validation of increased expression of five top In_SZCS-associated genes in SZ as compared to SZ_CON-like individuals, performed in RNA extracted from whole-cortex tissue samples of 13 SZ and five SZ_CON-like individuals within the McL cohort. Black dots indicate fold change of expression of each target gene in one SZ individual relative to average expression across all SZ_CON-like individuals normalized to 1, computed with the ΔΔct method and beta-2 microglobulin (*B2M*) used as the reference gene. Red dots indicate outlier values. (**F**) Enrichment of proteins localized to the synaptic compartment as annotated within the SynGO database (*45*) within the top 100 genes characterizing the merged Ex_SZCS and In_SZCS transcriptional signatures. 1, postsynaptic specialization; 2, postsynaptic density; 3, integral component of postsynaptic density membrane; 4, postsynaptic membrane; 5, extrinsic component of postsynaptic membrane; 6, integral component of postsynaptic membrane; 7, presynaptic active zone; 8, synaptic vesicle membrane; 9, integral component of synaptic active zone membrane; 10, presynaptic membrane; 11, integral component of presynaptic membrane.

the source of schizophrenia expression differences (17 of 65 individuals with schizophrenia and 22 of 75 healthy individuals) had TPSs of small magnitude, suggesting that discrepancy in classification stems from a low-assignment confidence and not a lack of reproducibility (gray points in off-diagonal quadrants in Fig. 6A).

To test whether discovered diagnostic subgroups could be explained by differences in underlying genetic risk, we next investigated the relationship between subgroups and genetic background. We computed polygenic risk scores (PRSs) for the subset of genotyped individuals of European ancestry (n = 99, 45 McL and 54 MSSM) and found a significant correlation between TPS and PRS (Pearson correlation = 0.26, P = 9.4e-3) and significantly different scores of each in individuals with schizophrenia versus healthy individuals (P < 1e-5, fig. S20), supporting a relationship between transcriptional pathology as defined herein and genetic risk. However, PRS was not different between SZ and SZ_CON-like, or

Corrected 6 August 2024. See full text.

between CON and CON_SZ-like groups (Fig. 6C), indicating that these groupings are not explained by known schizophrenia common variant genetic risk factors.

To better understand the gene signatures underlying diagnostic subgroups, we applied a matrix decomposition approach to simultaneously uncover hidden patterns of variability across all individuals and cells. Unlike TPS, this unbiased approach does not rely on prior knowledge of diagnosis but instead learns from the data transcriptional patterns that might recapitulate the observed individual-level heterogeneity of schizophrenia-associated transcriptional changes. The majority of transcriptional signatures identified corresponded to individual cell types, whereas four signatures were robustly expressed by cells within multiple neuronal populations, representing transcriptionally defined cellular states (fig. S21). One of these cellular states was marked by high expression of the *NRGN* gene and has been observed in prior snRNA-seq studies of human brain (*27*). The remaining three cellular states displayed contrasting associations with schizophrenia transcriptional changes.

Two of these cellular states displayed a positive association with TPS, with one marking excitatory neuronal populations (Ex_SZCS: excitatory schizophrenia cell state, R = 0.35, P = 1.9e-5) and the other inhibitory neurons (In_SZCS: inhibitory schizophrenia cell state, R = 0.56, P = 4.6e-13), whereas one cellular state (Ex_SZTR: excitatory schizophrenia transcriptional reversal) was negatively associated with TPS (R = −0.39, P = 1.8e-6). These associations were robust within the assembled cohort (Fig. 6D) and reproducible in each cohort independently (fig. S22). Although they marked distinct classes of neurons, In_SZCS and Ex_SZCS were highly correlated with respect to both the genes characterizing these transcriptional states (R = 0.6, P < 2.2e-16) and the individuals in which they were most prominently expressed (R = 0.7, P < 2.2e-16) (fig. S23). Both In_SZCS and Ex_SZCS were associated with diagnostic subgroups, with low average value in CON and in SZ_CON-like individuals and high average value in SZ and in CON_SZ-like individuals, with In_SZCS showing the strongest association. Ex_SZTR showed the opposite pattern, with high average value in SZ_CON-like and CON individuals (Fig. 6C, Fig. S24). Signatures of all three cellular states were correlated with TPS, but not with PRS (In_SZCS R = 4.3e-2, P = 6.6e-1, Ex_SZCS R=3.6e-2, P = 7.2e-1; Ex_SZTR R = −1.4e-1, P = 1.5e-1), suggesting an association with aspects of schizophrenia separate from known common genetic risk variants. Gene sets characterizing these three transcriptional states (datafile S12) were enriched for schizophrenia DEGs across multiple neuronal populations, with Ex_SZCS most strongly enriched for up-regulated and down-regulated DEGs within excitatory neurons, In_SZCS more strongly associated with DEGs in inhibitory neurons than the other cell states, and Ex_SZTR marked only by down-regulated DEGs across multiple excitatory neuronal populations (fig. S25).

Considering the similarities between Ex_SZCS and In_SZCS, we merged the sets of genes characterizing these transcriptional signatures for further investigation by first z-score normalizing each gene's specificity score, and then averaging the normalized scores across signatures. The gene most strongly associated with Ex_SZCS, In_SZCS, and both combined was *DHFR*, encoding dihydrofolate reductase, a key enzyme in one-carbon metabolism (*61*). Top genes characterizing the combined transcriptional signature also included *GRIN1*, encoding subunit 1 of the NMDA receptor; *EPHA6*, encoding a receptor tyrosine kinase implicated in axon guidance; *CHD5*, encoding a neuron-specific adenosine 5′-triphosphate (ATP)–dependent chromatin remodeling enzyme (*62*) with evidence of protein-coding mutations linked to schizophrenia risk (*13*); and *CNTNAP2*, encoding a neurexin protein necessary for clustering of potassium channels at nodes of Ranvier previously implicated in schizophrenia (*63*). Expression differences for these top genes between subgroups of individuals with schizophrenia were validated with qPCR, with all five tested genes showing increased expression in SZ as compared with SZ_CON-like individuals, as expected (Fig. 6E). More broadly, annotation of the top 100 merged cell state genes within the SynGO database (*45*) found strong evidence of overrepresentation of genes encoding proteins localized to both the presynaptic (GSEA P = 2.4e-13) and postsynaptic (GSEA P = 8.3e-17) compartments (Fig. 6F and fig. S26). These results suggest that among neuronal molecular processes associated with schizophrenia, expression of genes involved in one-carbon metabolism and neuronal depolarization (NMDA receptors, voltage-gated potassium channels), and enriched at the synapse, may indicate distinct molecular pathologies in subsets of individuals assigned a clinical diagnosis of schizophrenia.

Discussion

Here we present a robust and reproducible single-cell transcriptomic case-control dissection of schizophrenia across two datasets generated independently, with similar methodologies from distinct donor cohorts. We produced a high-resolution dataset of 468,727 single-cell transcriptomes sampled from 140 individuals and annotated 27 neuronal and glial cell types, which we used to investigate cell type–specific schizophrenia-dysregulated genes, pathways, and regulators. Although we observed changes in gene expression within all detected cell types, the majority of observed changes occurred in neuronal populations, with more than three-quarters of all observed changes occurring in excitatory neurons. DEGs were highly cell type–specific, with high concordance in direction of change within major cell classes and multiple divergently dysregulated DEGs. Transcriptomic signatures observed in bulk tissue studies (*20*) capture excitatory neuron DEGs, whereas transcriptional changes within inhibitory and non-neuronal populations are captured with less efficiency by bulk tissue measurements, highlighting the contribution of single-cell studies.

Functional assessment of schizophrenia DEGs identified downstream biological processes relevant to brain function, with neurodevelopment-relevant processes most strongly enriched and synaptic signaling pathways enriched across the greatest number of cell types. Schizophrenia DEGs further implicate a coherently expressed module of TFs, including multiple key neurodevelopmental regulatory factors (*64*) genetically associated with both schizophrenia and neurodevelopmental disorders. This recurrent theme of neurodevelopment within TFs and biological processes emerging from analyses of schizophrenia DEGs in adult brain tissue is relevant to the neurodevelopmental hypothesis of schizophrenia (*3*, *65*) and reflects that these regulators, classified as neurodevelopmental, also perform ongoing functions in the adult brain (*66*). We propose that the pleiotropic roles of these TFs may represent a link between early neurodevelopmental disruptions and adult brain function.

We observed an association between schizophrenia DEGs and both common genetic variants and rare protein-coding variants within excitatory neurons. Superficial layer excitatory populations showed considerable overlap in the implicated cell types, in keeping with the high similarity between the gene sets and pathways associated with these distinct categories of genetic risk (*13*). The strongest associations between schizophrenia DEGs and both categories of genetic risk variants occurred in excitatory neurons of deep cortical layers and unexpectedly implicated nonoverlapping populations, with Ex-L5*6* associated with common, and Ex-L6b_SEMA3E associated with rare, schizophrenia risk variants. If these discrepancies between the cell types most affected by schizophrenia risk variants at opposite ends of the population frequency spectrum are replicated by future larger studies, this may suggest potential roles for these cell types in mediating distinct categories of causal genetic effects.

We assessed transcriptomic heterogeneity across individuals within our cohorts and identified two subpopulations of individuals with schizophrenia, one being transcriptionally

similar to the schizophrenia group, and the other being more consistent with the healthy group, an observation consistent with analyses of large bulk tissue RNA-seq datasets (*60*). Although these groupings were not associated with PRS, they were well-captured by the expression of two related transcriptional signatures identified across all cells in the dataset blind to diagnosis. These transcriptional signatures, one expressed by excitatory neuronal populations (Ex_SZCS) and the other by inhibitory populations (In_SZCS), were characterized by high expression of schizophrenia DEGs observed within multiple neuronal cell types and by genes encoding proteins localized to the synapse.

There are multiple potential interpretations of the observed association between diagnostic subgroups and these transcriptional signatures, including medication effects, compensatory changes, or genetic associations not captured by common genetic variants. We did not observe an association between medication exposures within the cohort and either diagnostic subgroups or expression of Ex_SZCS or In_SZCS, and the observation of these transcriptional signatures within multiple healthy individuals also argues against them being an outcome of medication exposure or compensatory change. Top genes characterizing these transcriptional signatures encode key enzymes in one-carbon metabolism and chromatin modification, suggesting the possibility that they are related to nongenetic or environmental risk factors for schizophrenia. Interaction between one-carbon metabolism and schizophrenia pathology has long been hypothesized (*67*). Folate supplementation has been shown to reduce future risk of psychotic illness when administered during development (*68*) and to reduce schizophrenia symptoms when administered to adult individuals with schizophrenia (*69*).

In recent decades, substantial evidence has accumulated indicating that synaptic dysfunction plays a central role in the pathophysiology of schizophrenia, an observation now supported by immunohistochemistry (*70*), Golgi stain (*71*), and genetic association studies (*9*, *12*). Dysregulation of synapse-relevant genes and pathways was a recurrent observation across our analyses, further supporting synaptic dysfunction as central to the pathophysiology of schizophrenia. By mapping schizophrenia-associated changes in synaptic genes and pathways across the cytoarchitecture of the human PFC, our data may prove useful in the interpretation of emerging animal models of hyperactive or hypoactive synaptic pruning (*72*) and in guiding the design of mechanistic studies in human experimental systems with cell-type resolution.

Although this study provides numerous biological insights, the scope of this work is limited by multiple factors. Age of individuals was balanced across diagnostic groups and included in our DEG analysis, but the age range and size of the cohorts did not allow for robust secondary analysis of this variable. Future cohorts better powered to investigate the impact of age on diagnostic comparisons, as well as integration with data from studies of early developmental time points, may help disentangle the effects of causal genetic or environmental factors from those resulting from years of living with schizophrenia symptomatology. This work assessed isolated nuclei, and the differences between nuclear and whole-tissue RNA content must be considered in the interpretation of our findings. Also, although our case-control design is a strength of the study, this focus on human tissue does not allow experimental manipulation to investigate the causality of our observations, and experiments in model systems are needed. The direct observation of the cell type and direction of differential gene expression in disease-relevant human tissues adds valuable context to theories of disease mechanism; however, these data cannot determine whether such changes are a cause or a consequence of schizophrenia (*73*), or just correlations. Individuals with schizophrenia have very diverse experiences of treatment and clinical outcomes, and the presence of subgroups of individuals with schizophrenia suggested by our assessment of transcriptional signatures and cellular states is promising as an analytical approach to identify such subgroups more broadly in future studies.

The data presented here complement those from others in the field (*37*, *74*) and offer a cell type–specific reframing of schizophrenia transcriptional pathology by revealing specific cell populations affected by schizophrenia genes, variants, and regulators. Identification of pleiotropic transcriptional regulators linking developmental and adult schizophrenia-associated pathologies, contextualizing the outcome of known genetic risk factors within the human PFC, and discovery of transcriptional signatures associated with heterogeneity of schizophrenia molecular pathologies provide avenues for future research to unravel the genetic and environmental underpinnings of this complex and heterogeneous disease.

Materials and methods summary

Postmortem human brain tissue was collected by National Institute of Mental Health Neuro-BioBank associated tissue repositories, the Harvard Brain Tissue Resource Center at McLean Hospital (McL cohort, BA10), and the Mount Sinai/JJ Peters VA Medical Center NIH Brain and Tissue Repository (MSSM cohort, BA9, 10, or 46). Single-nucleus RNA-seq was performed in each cohort independently at the respective site using 10x Genomics Chromium Single Cell 3′ Reagent Kits v3 with sample multiplexing. The McL cohort was assayed in batches of nine samples using nuclear hashing with sample-specific cholesterol-conjugated oligonucleotides (Integrated DNA Technologies) per the MULTI-Seq (*75*) protocol. The MSSM cohort was assayed in batches of six samples multiplexed with sample-specific TotalSeq-A nuclear hashing antibodies (BioLegend). 10x Genomics and hashtag libraries were prepared using standard protocols (*76*). Gene count matrices were generated by aligning reads (including intronic reads) to the hg38 genome using 10x Genomics Cell Ranger software v3.0.1. Hashtag FASTQ files were processed using the deMULTIplex R package (*75*) and the Seurat R package (*77*) to determine the subject of origin for each captured nucleus, as well as to identify intersample doublets. We further applied the doublet detection tool Scrublet (*78*) to predict and remove additional potential doublet cells. Only cells passing a stringent, multistep quality control protocol were considered for downstream analyses. Cell annotation and clustering were performed across all retained cells in both cohorts together using ACTIONet (*79*).

Differential gene expression analysis was conducted in each cohort separately and then combined using a meta-analysis approach. Pseudobulk gene expression profiles with log-transformed expression counts were assessed with the multisample multigroup scRNA-seq data analysis tools (muscat) R package (*80*). DE analyses were performed separately for each cohort and cell type, after removing the effect of batch and HTO variables using the removeBatchEffect function in limma (*81*), while incorporating age, sex, postmortem interval, and the log transform of the average number of UMIs captured per cell as covariates. Differential expression meta-analysis was performed over all genes via a fixed-effects meta-analysis (*82*) in each of the 25 cell types robustly captured in both cohorts. FDR multiple testing correction was performed over all combined genes in each cell type independently, with FDR-corrected $P < 0.05$ and absolute logFC > 0.1 considered significant. Validation of cell-type annotations was performed with in situ hybridization in three frozen BA10 tissue blocks from unaffected control donors using probes and reagents from Advanced Cell Diagnostics to characterize subpopulations of Rosehip interneurons. Validation of differential gene expression between the schizophrenia and unaffected control groups, and between the SZ and SZ_CON-like groups, was performed by qPCR with primer sets from Integrated DNA Technologies. Association of prioritized TFs with schizophrenia DEGs was validated with CUT&Tag experiments performed in neuronal nuclei isolated from postmortem human PFC with

Corrected 6 August 2024. See full text.

fluorescence-activated nuclear sorting, and CUT&Tag signal enrichment was assessed by peak calling using Sparse Enrichment for CUT&Run (*83*). A stringent set of reproducibly bound regions was defined with binding support in at least 50% of samples, and the overrepresentation of DEGs within the genes annotated to these reproducibly bound regions using the ChIPseeker R package (*84*) was tested using the Fisher's exact test.

TPS scores were produced within each cell type by computing the partial Pearson's correlation between the expression profile of each individual and the meta-analysis differential expression profile observed between the schizophrenia and healthy groups, after correcting for the mean expression of genes in the given cell type. Each individual's aggregate TPS was defined as the average TPS across all neuronal cell types for that individual.

Cell state analysis was performed using ACTIONet (*79*) to identify a set of dominant transcriptional patterns explaining the heterogeneity across all cells and all individuals in the dataset. A single-value decomposition-based preprocessing step first produced a low-rank approximation of the normalized count matrix, and this reduced data representation was subsequently decomposed multiple times using an archetypal analysis–based approach with increasing resolution (number of archetypes) to define a multiresolution and low-dimensional cell state representation for each individual cell, producing a matrix of archetypes (cell states) and a matrix of cell encodings. See the supplementary materials and methods for full details.

REFERENCES AND NOTES

1. R. S. Kahn *et al*., Schizophrenia. *Nat. Rev. Dis. Primers* **1**, 15067 (2015). doi: 10.1038/nrdp.2015.67; pmid: 27189524
2. J. K. Forsyth, D. A. Lewis, Mapping the Consequences of Impaired Synaptic Plasticity in Schizophrenia through Development: An Integrative Model for Diverse Clinical Features. *Trends Cogn. Sci.* **21**, 760–778 (2017). doi: 10.1016/j.tics.2017.06.006; pmid: 28754595
3. D. R. Weinberger, Future of Days Past: Neurodevelopment and Schizophrenia. *Schizophr. Bull.* **43**, 1164–1168 (2017). doi: 10.1093/schbul/sbx118; pmid: 29040792
4. J. T. Glessner *et al*., Strong synaptic transmission impact by copy number variations in schizophrenia. *Proc. Natl. Acad. Sci. U.S.A.* **107**, 10584–10589 (2010). doi: 10.1073/pnas.1000274107; pmid: 20489179
5. E. Schwarz, R. Izmailov, P. Liò, A. Meyer-Lindenberg, Protein Interaction Networks Link Schizophrenia Risk Loci to Synaptic Function. *Schizophr. Bull.* **42**, 1334–1342 (2016). doi: 10.1093/schbul/sbw035; pmid: 27056717
6. E. Nanou, W. A. Catterall, Calcium Channels, Synaptic Plasticity, and Neuropsychiatric Disease. *Neuron* **98**, 466–481 (2018). doi: 10.1016/j.neuron.2018.03.017;pmid: 29723500
7. T. Mäki-Marttunen *et al*., Functional Effects of Schizophrenia-Linked Genetic Variants on Intrinsic Single-Neuron Excitability: A Modeling Study. *Biol. Psychiatry Cogn. Neurosci. Neuroimaging* **1**, 49–59 (2016). doi: 10.1016/j.bpsc.2015.09.002; pmid: 26949748
8. H. Cao, H. Zhou, T. D. Cannon, Functional connectome-wide associations of schizophrenia polygenic risk. *Mol. Psychiatry* **26**, 2553–2561 (2021). doi: 10.1038/s41380-020-0699-3; pmid: 32127647
9. A. Sekar *et al*., Schizophrenia risk from complex variation of complement component 4. *Nature* **530**, 177–183 (2016). doi: 10.1038/nature16549; pmid: 26814963
10. R. S. Kahn, R. S. E. Keefe, Schizophrenia is a cognitive illness: Time for a change in focus. *JAMA Psychiatry* **70**, 1107–1112 (2013). doi: 10.1001/jamapsychiatry.2013.155; pmid: 23925787
11. T. Toulopoulou *et al*., Polygenic risk score increases schizophrenia liability through cognition-relevant pathways. *Brain* **142**, 471–485 (2019). doi: 10.1093/brain/awy279; pmid: 30535067
12. V. Trubetskoy *et al*., Mapping genomic loci implicates genes and synaptic biology in schizophrenia. *Nature* **604**, 502–508 (2022). doi: 10.1038/s41586-022-04434-5; pmid: 35396580
13. T. Singh *et al*., Rare coding variants in ten genes confer substantial risk for schizophrenia. *Nature* **604**, 509–516 (2022). doi: 10.1038/s41586-022-04556-w; pmid: 35396579
14. S. E. Hemby *et al*., Gene expression profile for schizophrenia: Discrete neuron transcription patterns in the entorhinal cortex. *Arch. Gen. Psychiatry* **59**, 631–640 (2002). doi: 10.1001/archpsyc.59.7.631; pmid: 12090816
15. J. F. Enwright Iii *et al*., Transcriptome alterations of prefrontal cortical parvalbumin neurons in schizophrenia. *Mol. Psychiatry* **23**, 1606–1613 (2018). doi: 10.1038/mp.2017.216; pmid: 29112193
16. A. E. Jaffe *et al*., Profiling gene expression in the human dentate gyrus granule cell layer reveals insights into schizophrenia and its genetic risk. *Nat. Neurosci.* **23**, 510–519 (2020). doi: 10.1038/s41593-020-0604-z; pmid: 32203495
17. W. B. Ruzicka *et al*., Selective epigenetic alteration of layer I GABAergic neurons isolated from prefrontal cortex of schizophrenia patients using laser-assisted microdissection. *Mol. Psychiatry* **12**, 385–397 (2007). doi: 10.1038/sj.mp.4001954; pmid: 17264840
18. W. B. Ruzicka, S. Subburaju, F. M. Benes, Circuit- and Diagnosis-Specific DNA Methylation Changes at γ-Aminobutyric Acid-Related Genes in Postmortem Human Hippocampus in Schizophrenia and Bipolar Disorder. *JAMA Psychiatry* **72**, 541–551 (2015). doi: 10.1001/jamapsychiatry.2015.49; pmid: 25738424
19. F. M. Benes *et al*., Regulation of the GABA cell phenotype in hippocampus of schizophrenics and bipolars. *Proc. Natl. Acad. Sci. U.S.A.* **104**, 10164–10169 (2007). doi: 10.1073/pnas.0703806104; pmid: 17553960
20. M. J. Gandal *et al*., Transcriptome-wide isoform-level dysregulation in ASD, schizophrenia, and bipolar disorder. *Science* **362**, eaat8127 (2018). doi: 10.1126/science.aat8127; pmid: 30545856
21. G. E. Hoffman *et al*., CommonMind Consortium provides transcriptomic and epigenomic data for Schizophrenia and Bipolar Disorder. *Sci. Data* **6**, 180 (2019). doi: 10.1038/s41597-019-0183-6; pmid: 31551426
22. I. Mendizabal *et al*., Cell type-specific epigenetic links to schizophrenia risk in the brain. *Genome Biol.* **20**, 135 (2019). doi: 10.1186/s13059-019-1747-7; pmid: 31288836
23. K. Girdhar *et al*., Chromatin domain alterations linked to 3D genome organization in a large cohort of schizophrenia and bipolar disorder brains. *Nat. Neurosci.* **25**, 474–483 (2022). doi: 10.1038/s41593-022-01032-6; pmid: 35332326
24. G. X. Y. Zheng *et al*., Massively parallel digital transcriptional profiling of single cells. *Nat. Commun.* **8**, 14049 (2017). doi: 10.1038/ncomms14049; pmid: 28091601
25. S. Aldridge, S. A. Teichmann, Single cell transcriptomics comes of age. *Nat. Commun.* **11**, 4307 (2020). doi: 10.1038/s41467-020-18158-5; pmid: 32855414
26. H. Mathys *et al*., Single-cell transcriptomic analysis of Alzheimer's disease. *Nature* **570**, 332–337 (2019). doi: 10.1038/s41586-019-1195-2; pmid: 31042697
27. D. Velmeshev *et al*., Single-cell genomics identifies cell type-specific molecular changes in autism. *Science* **364**, 685–689 (2019). doi: 10.1126/science.aav8130; pmid: 31097668
28. C. Nagy *et al*., Single-nucleus transcriptomics of the prefrontal cortex in major depressive disorder implicates oligodendrocyte precursor cells and excitatory neurons. *Nat. Neurosci.* **23**, 771–781 (2020). doi: 10.1038/s41593-020-0621-y; pmid: 32341540
29. M. Maitra *et al*., Cell type specific transcriptomic differences in depression show similar patterns between males and females but implicate distinct cell types and genes. *Nat. Commun.* **14**, 2912 (2023). doi: 10.1038/s41467-023-38530-5; pmid: 37217515
30. D. Schafflick *et al*., Integrated single cell analysis of blood and cerebrospinal fluid leukocytes in multiple sclerosis. *Nat. Commun.* **11**, 247 (2020). doi: 10.1038/s41467-019-14118-w; pmid: 31937773
31. S. Mohammadi, J. Davila-Velderrain, M. Kellis, A multiresolution framework to characterize single-cell state landscapes. *Nat. Commun.* **11**, 5399 (2020). doi: 10.1038/s41467-020-18416-6; pmid: 33106496
32. E. Boldog *et al*., Transcriptomic and morphophysiological evidence for a specialized human cortical GABAergic cell type. *Nat. Neurosci.* **21**, 1185–1195 (2018). doi: 10.1038/s41593-018-0205-2; pmid: 30150662
33. A. Kepecs, G. Fishell, Interneuron cell types are fit to function. *Nature* **505**, 318–326 (2014). doi: 10.1038/nature12983; pmid: 24429630
34. F. M. Benes, J. McSparren, E. D. Bird, J. P. SanGiovanni, S. L. Vincent, Deficits in small interneurons in prefrontal and cingulate cortices of schizophrenic and schizoaffective patients. *Arch. Gen. Psychiatry* **48**, 996–1001 (1991). doi: 10.1001/archpsyc.1991.01810350036005; pmid: 1747023
35. C. L. Beasley, Z. J. Zhang, I. Patten, G. P. Reynolds, Selective deficits in prefrontal cortical GABAergic neurons in schizophrenia defined by the presence of calcium-binding proteins. *Biol. Psychiatry* **52**, 708–715 (2002). doi: 10.1016/S0006-3223(02)01360-4; pmid: 12372661
36. J. F. Enwright *et al*., Reduced Labeling of Parvalbumin Neurons and Perineuronal Nets in the Dorsolateral Prefrontal Cortex of Subjects with Schizophrenia. *Neuropsychopharmacology* **41**, 2206–2214 (2016). doi: 10.1038/npp.2016.24; pmid: 26868058
37. M. Y. Batiuk *et al*., Upper cortical layer-driven network impairment in schizophrenia. *Sci. Adv.* **8**, eabn8367 (2022). doi: 10.1126/sciadv.abn8367; pmid: 36223459
38. K. R. Maynard *et al*., Transcriptome-scale spatial gene expression in the human dorsolateral prefrontal cortex. *Nat. Neurosci.* **24**, 425–436 (2021). doi: 10.1038/s41593-020-00787-0; pmid: 33558695
39. N. G. Skene *et al*., Genetic identification of brain cell types underlying schizophrenia. *Nat. Genet.* **50**, 825–833 (2018). doi: 10.1038/s41588-018-0129-5; pmid: 29785013
40. A. Tromp, B. Mowry, J. Giacomotto, Neurexins in autism and schizophrenia-a review of patient mutations, mouse models and potential future directions. *Mol. Psychiatry* **26**, 747–760 (2021). doi: 10.1038/s41380-020-00944-8; pmid: 33191396
41. C. R. Sullivan *et al*., Connectivity Analyses of Bioenergetic Changes in Schizophrenia: Identification of Novel Treatments. *Mol. Neurobiol.* **56**, 4492–4517 (2019). doi: 10.1007/s12035-018-1390-4; pmid: 30338483
42. B. Schwechter, C. Rosenmund, K. F. Tolias, RasGRF2 Rac-GEF activity couples NMDA receptor calcium flux to enhanced synaptic transmission. *Proc. Natl. Acad. Sci. U.S.A.* **110**, 14462–14467 (2013). doi: 10.1073/pnas.1304340110; pmid: 23940355
43. S. Peykov *et al*., Identification and functional characterization of rare SHANK2 variants in schizophrenia. *Mol. Psychiatry* **20**, 1489–1498 (2015). doi: 10.1038/mp.2014.172; pmid: 25560758
44. S.-H. J. Wang *et al*., Dlg5 regulates dendritic spine formation and synaptogenesis by controlling subcellular N-cadherin localization. *J. Neurosci.* **34**, 12745–12761 (2014). doi: 10.1523/JNEUROSCI.1280-14.2014; pmid: 25232112
45. F. Koopmans *et al*., SynGO: An Evidence-Based, Expert-Curated Knowledge Base for the Synapse. *Neuron* **103**, 217–234.e4 (2019). doi: 10.1016/j.neuron.2019.05.002; pmid: 31171447
46. X. Liu, Y. I. Li, J. K. Pritchard, Trans Effects on Gene Expression Can Drive Omnigenic Inheritance. *Cell* **177**, 1022–1034.e6 (2019). doi: 10.1016/j.cell.2019.04.014; pmid: 31051098
47. D. Szklarczyk *et al*., STRING v11: Protein-protein association networks with increased coverage, supporting functional discovery in genome-wide experimental datasets. *Nucleic Acids Res.* **47**, D607–D613 (2019). doi: 10.1093/nar/gky1131; pmid: 30476243
48. M. Wang, Y. Zhao, B. Zhang, Efficient Test and Visualization of Multi-Set Intersections. *Sci. Rep.* **5**, 16923 (2015). doi: 10.1038/srep16923; pmid: 26603754
49. J. M. Fu *et al*., Rare coding variation provides insight into the genetic architecture and phenotypic context of autism. *Nat. Genet.* **54**, 1320–1331 (2022). doi: 10.1038/s41588-022-01104-0; pmid: 35982160
50. H. S. Kaya-Okur *et al*., CUT&Tag for efficient epigenomic profiling of small samples and single cells. *Nat. Commun.* **10**, 1930 (2019). doi: 10.1038/s41467-019-09982-5; pmid: 31036827
51. N. Y. A. Sey *et al*., A computational tool (H-MAGMA) for improved prediction of brain-disorder risk genes by incorporating brain chromatin interaction profiles. *Nat. Neurosci.* **23**, 583–593 (2020). doi: 10.1038/s41593-020-0603-0; pmid: 32152537

52. D. Wang *et al*., Comprehensive functional genomic resource and integrative model for the human brain. *Science* **362**, eaat8464 (2018). doi: 10.1126/science.aat8464; pmid: 30545857
53. C. A. de Leeuw, J. M. Mooij, T. Heskes, D. Posthuma, MAGMA: Generalized gene-set analysis of GWAS data. *PLOS Comput. Biol.* **11**, e1004219 (2015). doi: 10.1371/journal.pcbi.1004219; pmid: 25885710
54. D. Cameron *et al*., Single-Nuclei RNA Sequencing of 5 Regions of the Human Prenatal Brain Implicates Developing Neuron Populations in Genetic Risk for Schizophrenia. *Biol. Psychiatry* **93**, 157–166 (2023). doi: 10.1016/j.biopsych.2022.06.033; pmid: 36150908
55. D. M. Howard *et al*., Genome-wide meta-analysis of depression identifies 102 independent variants and highlights the importance of the prefrontal brain regions. *Nat. Neurosci.* **22**, 343–352 (2019). doi: 10.1038/s41593-018-0326-7; pmid: 30718901
56. E. A. Stahl *et al*., Genome-wide association study identifies 30 loci associated with bipolar disorder. *Nat. Genet.* **51**, 793–803 (2019). doi: 10.1038/s41588-019-0397-8; pmid: 31043756
57. J. Grove *et al*., Identification of common genetic risk variants for autism spectrum disorder. *Nat. Genet.* **51**, 431–444 (2019). doi: 10.1038/s41588-019-0344-8; pmid: 30804558
58. I. E. Jansen *et al*., Genome-wide meta-analysis identifies new loci and functional pathways influencing Alzheimer's disease risk. *Nat. Genet.* **51**, 404–413 (2019). doi: 10.1038/s41588-018-0311-9; pmid: 30617256
59. S. H. Lee *et al*., Genetic relationship between five psychiatric disorders estimated from genome-wide SNPs. *Nat. Genet.* **45**, 984–994 (2013). doi: 10.1038/ng.2711; pmid: 23933821
60. E. F. W. Bowen, J. L. Burgess, R. Granger, J. E. Kleinman, C. H. Rhodes, DLPFC transcriptome defines two molecular subtypes of schizophrenia. *Transl. Psychiatry* **9**, 147 (2019). doi: 10.1038/s41398-019-0472-z; pmid: 31073119
61. C. E. Clare, A. H. Brassington, W. Y. Kwong, K. D. Sinclair, One-Carbon Metabolism: Linking Nutritional Biochemistry to Epigenetic Programming of Long-Term Development. *Annu. Rev. Anim. Biosci.* **7**, 263–287 (2019). doi: 10.1146/annurev-animal-020518-115206; pmid: 30412672
62. P. Deloukas *et al*., The DNA sequence and comparative analysis of human chromosome 20. *Nature* **414**, 865–871 (2001). doi: 10.1038/414865a; pmid: 11780052
63. C. Toma *et al*., Comprehensive cross-disorder analyses of CNTNAP2 suggest it is unlikely to be a primary risk gene for psychiatric disorders. *PLOS Genet.* **14**, e1007535 (2018). doi: 10.1371/journal.pgen.1007535; pmid: 30586385
64. M. Li *et al*., Integrative functional genomic analysis of human brain development and neuropsychiatric risks. *Science* **362**, eaat7615 (2018). doi: 10.1126/science.aat7615; pmid: 30545854
65. R. Birnbaum, D. R. Weinberger, Genetic insights into the neurodevelopmental origins of schizophrenia. *Nat. Rev. Neurosci.* **18**, 727–740 (2017). doi: 10.1038/nrn.2017.125; pmid: 29070826
66. G. Maussion *et al*., Investigation of genes important in neurodevelopment disorders in adult human brain. *Hum. Genet.* **134**, 1037–1053 (2015). doi: 10.1007/s00439-015-1584-z; pmid: 26194112
67. F. R. Frankenburg, The role of one-carbon metabolism in schizophrenia and depression. *Harv. Rev. Psychiatry* **15**, 146–160 (2007). doi: 10.1080/10673220701551136; pmid: 17687709
68. H. Eryilmaz *et al*., Association of Prenatal Exposure to Population-Wide Folic Acid Fortification With Altered Cerebral Cortex Maturation in Youths. *JAMA Psychiatry* **75**, 918–928 (2018). doi: 10.1001/jamapsychiatry.2018.1381; pmid: 29971329
69. J. L. Roffman *et al*., Biochemical, physiological and clinical effects of l-methylfolate in schizophrenia: A randomized controlled trial. *Mol. Psychiatry* **23**, 316–322 (2018). doi: 10.1038/mp.2017.41; pmid: 28289280
70. S. L. Eastwood, P. J. Harrison, Decreased expression of vesicular glutamate transporter 1 and complexin II mRNAs in schizophrenia: Further evidence for a synaptic pathology affecting glutamate neurons. *Schizophr. Res.* **73**, 159–172 (2005). doi: 10.1016/j.schres.2004.05.010; pmid: 15653259
71. N. Kolluri, Z. Sun, A. R. Sampson, D. A. Lewis, Lamina-specific reductions in dendritic spine density in the prefrontal cortex of subjects with schizophrenia. *Am. J. Psychiatry* **162**, 1200–1202 (2005). doi: 10.1176/appi.ajp.162.6.1200; pmid: 15930070
72. M. Yilmaz *et al*., Overexpression of schizophrenia susceptibility factor human complement C4A promotes excessive synaptic loss and behavioral changes in mice. *Nat. Neurosci.* **24**, 214–224 (2021). doi: 10.1038/s41593-020-00763-8; pmid: 33353966
73. M. E. Hauberg *et al*., Large-Scale Identification of Common Trait and Disease Variants Affecting Gene Expression. *Am. J. Hum. Genet.* **101**, 157 (2017). doi: 10.1016/j.ajhg.2017.06.003; pmid: 28686855
74. B. C. Reiner *et al*., Single-nuclei transcriptomics of schizophrenia prefrontal cortex primarily implicates neuronal subtypes. *bioRxiv* (2021), p. 2020.07.29.227355.
75. C. S. McGinnis *et al*., MULTI-seq: Sample multiplexing for single-cell RNA sequencing using lipid-tagged indices. *Nat. Methods* **16**, 619–626 (2019). doi: 10.1038/s41592-019-0433-8; pmid: 31209384
76. M. Stoeckius *et al*., Cell Hashing with barcoded antibodies enables multiplexing and doublet detection for single cell genomics. *Genome Biol.* **19**, 224 (2018). doi: 10.1186/s13059-018-1603-1; pmid: 30567574
77. A. Butler, P. Hoffman, P. Smibert, E. Papalexi, R. Satija, Integrating single-cell transcriptomic data across different conditions, technologies, and species. *Nat. Biotechnol.* **36**, 411–420 (2018). doi: 10.1038/nbt.4096; pmid: 29608179
78. S. L. Wolock, R. Lopez, A. M. Klein, Scrublet: Computational Identification of Cell Doublets in Single-Cell Transcriptomic Data. *Cell Syst.* **8**, 281–291.e9 (2019). doi: 10.1016/j.cels.2018.11.005; pmid: 30954476
79. S. Mohammadi, J. Davila-Velderrain, M. Kellis, A multiresolution framework to characterize single-cell state landscapes. *Nat. Commun.* **11**, 5399 (2020). doi: 10.1038/s41467-020-18416-6; pmid: 33106496
80. H. L. Crowell *et al*., muscat detects subpopulation-specific state transitions from multi-sample multi-condition single-cell transcriptomics data. *Nat. Commun.* **11**, 6077 (2020). doi: 10.1038/s41467-020-19894-4; pmid: 33257685
81. M. E. Ritchie *et al*., limma powers differential expression analyses for RNA-sequencing and microarray studies. *Nucleic Acids Res.* **43**, e47 (2015). doi: 10.1093/nar/gkv007; pmid: 25605792
82. W. Viechtbauer, Conducting Meta-Analyses in R with the metafor Package. *J. Stat. Softw.* **36**, 1–48 (2010). doi: 10.18637/jss.v036.i03
83. M. P. Meers, D. Tenenbaum, S. Henikoff, Peak calling by Sparse Enrichment Analysis for CUT&RUN chromatin profiling. *Epigenetics Chromatin* **12**, 42 (2019). doi: 10.1186/s13072-019-0287-4; pmid: 31300027
84. G. Yu, L.-G. Wang, Q.-Y. He, ChIPseeker: An R/Bioconductor package for ChIP peak annotation, comparison and visualization. *Bioinformatics* **31**, 2382–2383 (2015). doi: 10.1093/bioinformatics/btv145; pmid: 25765347
85. Z. He *et al*., Comprehensive transcriptome analysis of neocortical layers in humans, chimpanzees and macaques. *Nat. Neurosci.* **20**, 886–895 (2017). doi: 10.1038/nn.4548; pmid: 28414332
86. A. B. Keenan *et al*., ChEA3: Transcription factor enrichment analysis by orthogonal omics integration. *Nucleic Acids Res.* **47**, W212–W224 (2019). doi: 10.1093/nar/gkz446; pmid: 31114921

ACKNOWLEDGMENTS

We thank the individuals and families whose donation of human brain tissue made this work possible. **Funding:** National Institutes of Health grant K08MH109759 to W.B.R. National Institutes of Health grant R01AG050986 to P.R. National Institutes of Health grant R01MH109677 to P.R. National Institutes of Health grant U01MH116442 to P.R. National Institutes of Health grant R01MH110921 to P.R. National Institutes of Health grant R01MH125246 to P.R. National Institutes of Health grant R01AG067025 to P.R. Veterans Affairs Merit grant BX002395 to P.R. National Institutes of Health grant 1U01MH119509 to M.K. National Institutes of Health grant R01MH109978 to M.K. National Institutes of Health grant R01AG062335 to M.K. National Institutes of Health grant K08MH122911 to G.V. National Institutes of Health grant HHSN271201300031C to V.H. Data were generated as part of the PsychENCODE Consortium, supported by U01DA048279, U01MH103339, U01MH103340, U01MH103346, U01MH103365, U01MH103392, U01MH116438, U01MH116441, U01MH116442, U01MH116488, U01MH116489, U01MH116492, U01MH122590, U01MH122591, U01MH122592, U01MH122849, U01MH122678, U01MH122681, U01MH116487, U01MH122509, R01MH094714, R01MH105472, R01MH105898, R01MH109677, R01MH109715, R01MH110905, R01MH110920, R01MH110921, R01MH110926, R01MH110927, R01MH110928, R01MH111721, R01MH117291, R01MH117292, R01MH117293, R21MH102791, R21MH103877, R21MH105853, R21MH105881, R21MH109956, R56MH114899, R56MH114901, R56MH114911, R01MH125516, R01MH126459, R01MH129301, R01MH126393, R01MH121521, R01MH116529, R01MH129817, R01MH117406, and P50MH106934 awarded to A. Abyzov, N. Ahituv, S. Akbarian, K. Brennand, A. Chess, G. Cooper, G. Crawford, S. Dracheva, P. Farnham, M. Gandal, M. Gerstein, D. Geschwind, F. Goes, J. F. Hallmayer, V. Haroutunian, T. M. Hyde, A. Jaffe, P. Jin, M. Kellis, J. Kleinman, J. A. Knowles, A. Kriegstein, C. Liu, C. E. Mason, K. Martinowich, E. Mukamel, R. Myers, C. Nemeroff, M. Peters, D. Pinto, K. Pollard, K. Ressler, P. Roussos, S. Sanders, N. Sestan, P. Sklar, M. P. Snyder, M. State, J. Stein, P. Sullivan, A. E. Urban, F. Vaccarino, S. Warren, D. Weinberger, S. Weissman, Z. Weng, K. White, A. J. Willsey, H. Won, and P. Zandi. **Author contributions:** Conceptualization: W.B.R., J.F.F., P.R. Methodology: W.B.R., J.F.F. Investigation: W.B.R., J.F.F., S.S., D.R.T., M.H. Data curation: W.B.R., S.J., H.-C.L. Software: S.M., J.D.-V. Visualization: W.B.R., S.M., J.D.-V. Formal Analysis: S.M., J.D., J.B., G.V., G.E.H. Resources: W.B.R., V.H., P.R., M.K. Supervision: W.B.R., P.R., M.K. Funding acquisition: M.K., P.R., W.B.R., G.V., V.H. Writing - original draft: W.B.R., S.M., J.D.-V. Writing - review and editing: W.B.R., S.M., J.F.F., J.D.-V., G.E.H., P.R., M.K. **Competing interests:** The authors declare that they have no competing interests. **Data and materials availability:** The source data and processed datasets described in this manuscript are available via the PsychENCODE Knowledge Portal (https://psychencode.org), a platform for accessing data, analyses, and tools generated through grants funded by the National Institute of Mental Health's PsychENCODE program. For access to content described in this manuscript, see https://doi.org/10.7303/syn25922167. **License information:** Copyright © 2024 the authors, some rights reserved; exclusive licensee American Association for the Advancement of Science. No claim to original US government works. https://www.sciencemag.org/about/science-licenses-journal-article-reuse

SUPPLEMENTARY MATERIALS

Submitted 2 February 2023; accepted 21 July 2023
10.1126/science.adg5136

Single-cell multi-cohort dissection of the schizophrenia transcriptome

W. Brad Ruzicka, Shahin Mohammadi, John F. Fullard, Jose Davila-Velderrain, Sivan Subburaju, Daniel Reed Tso, Makayla Hourihan, Shan Jiang, Hao-Chih Lee, Jaroslav Bendl, PsychENCODE Consortium, Georgios Voloudakis, Vahram Haroutunian, Gabriel E. Hoffman, Panos Roussos, Manolis Kellis, Schahram Akbarian, Alexej Abyzov, Nadav Ahituv, Dhivya Arasappan, Jose Juan Almagro Armenteros, Brian J. Beliveau, Sabina Berretta, Rahul A. Bharadwaj, Arjun Bhattacharya, Lucy Bicks, Kristen Brennand, Davide Capauto, Frances A. Champagne, Tanima Chatterjee, Chris Chatzinakos, Yuhang Chen, H. Isaac Chen, Yuyan Cheng, Lijun Cheng, Andrew Chess, Jo-fan Chien, Zhiyuan Chu, Declan Clarke, Ashley Clement, Leonardo Collado-Torres, Gregory M. Cooper, Gregory E. Crawford, Rujia Dai, Nikolaos P. Daskalakis, Amy Deep-Soboslay, Chengyu Deng, Christopher P. DiPietro, Stella Dracheva, Shiron Drusinsky, Ziheng Duan, Duc Duong, Cagatay Dursun, Nicholas J. Eagles, Jonathan Edelstein, Prashant S. Emani, Kiki Galani, Timur Galeev, Michael J. Gandal, Sophia Gaynor, Mark Gerstein, Daniel H. Geschwind, Kiran Girdhar, Fernando S. Goes, William Greenleaf, Jennifer Grundman, Hanmin Guo, Qiuyu Guo, Chirag Gupta, Yoav Hadas, Joachim Hallmayer, Xikun Han, Natalie Hawken, Chuan He, Ella Henry, Stephanie C. Hicks, Marcus Ho, Li-Lun Ho, Yiling Huang, Louise A. Huuki-Myers, Ahyeon Hwang, Thomas M. Hyde, Artemis Iatrou, Fumitaka Inoue, Aarti Jajoo, Matthew Jensen, Lihua Jiang, Peng Jin, Ting Jin, Connor Jops, Alexandre Jourdon, Riki Kawaguchi, Joel E. Kleinman, Steven P. Kleopoulos, Alex Kozlenkov, Arnold Kriegstein, Anshul Kundaje, Soumya Kundu, Cheyu Lee, Donghoon Lee, Junhao Li, Mingfeng Li, Xiao Lin, Shuang Liu, Jason Liu, Jianyin Liu, Chunyu Liu, Shuang Liu, Shaoke Lou, Jacob M. Loupe, Dan Lu, Shaojie Ma, Liang Ma, Michael Margolis, Jessica Mariani, Keri Martinowich, Kristen R. Maynard, Samantha Mazariegos, Ran Meng, Richard M. Myers, Courtney Micallef, Tatiana Mikhailova, Guo-li Ming, Emma Monte, Kelsey S. Montgomery, Jill E. Moore, Jennifer R. Moran, Eran A. Mukamel, Angus C. Nairn, Charles B. Nemeroff, Pengyu Ni, Scott Norton, Tomasz Nowakowski, Larsson Omberg, Stephanie C. Page, Saejeong Park, Ashok Patowary, Reenal Pattni, Geo Pertea, Mette A. Peters, Nishigandha Phalke, Dalila Pinto, Milos Pjanic, Sirisha Pochareddy, Katherine S. Pollard, Alex Pollen, Henry Pratt, Pawel F. Przytycki, Carolin Purmann, Zhaohui S. Qin, Ping-Ping Qu, Diana Quintero, Towfique Raj, Ananya S. Rajagopalan, Sarah Reach, Thomas Reimonn, Kerry J. Ressler, Deanna Ross, Joel Rozowsky, Misir Ruth, Stephan J. Sanders, Juliane M. Schneider, Soraya Scuderi, Robert Sebra, Nenad Sestan, Nicholas Seyfried, Zhiping Shao, Nicole Shedd, Annie W. Shieh, Joo Heon Shin, Mario Skarica, Clara Snijders, Hongjun Song, Matthew W. State, Jason Stein, Marilyn Steyert, Thomas Sudhof, Michael Snyder, Ran Tao, Karen Therrien, Li-Huei Tsai, Alexander E. Urban, Flora M. Vaccarino, Harm van Bakel, Daniel Vo, Brie Wamsley, Tao Wang, Sidney H. Wang, Daifeng Wang, Yifan Wang, Jonathan Warrell, Yu Wei, Annika K. Weimer, Daniel R. Weinberger, Cindy Wen, Zhiping Weng, Sean Whalen, Kevin P. White, A. Jeremy Willsey, Hyejung Won, Wing Wong, Hao Wu, Feinan Wu, Stefan Wuchty, Dennis Wylie, Siwei Xu, Chloe X. Yap, Biao Zeng, Pan Zhang, Chunling Zhang, Bin Zhang, Jing Zhang, Yanqiong Zhang, Xiao Zhou, Ryan Ziffra, Zane R. Zeier, and Trisha M. Zintel

Science **384** (6698), eadg5136. DOI: 10.1126/science.adg5136